

Fig. 4. Analysis of miRNA expression data. Target genes of miRNAs were predicted using MIRANDA Pro3.0; candidate target genes spotted on microarray were identified; number of genes that actually exhibit significant ($P < 0.05$) changes in expression among the genes was determined; and signal pathways involving genes regulated by the miRNAs that had exhibited differential expression between each group were analyzed using MetaCore (Table 4).

noting that the prediction rate may be likely an overestimate of the true rate, given the weaknesses of cross-validation and bootstrapping methods in a strict sense.)

Microarray Analysis. cDNA microarray slides (Liver chip 10k) were used as described.¹⁰ RNA isolation, amplification of antisense RNA, labeling, and hybridization were performed according to the protocols described.^{9,10} Quantitative assessment of the signals on the slides was performed by scanning on the ScanArray 5000 (General Scanning, Watertown, MA) followed by image analysis using GenePix Pro 4.1 (Axon Instruments, Union City, CA) as described.¹⁰

Preliminary Survey of Independency of Paired Samples from the Same Patient. CH and HCC expression data were derived from the same patient. Before further analysis, we examined whether the miRNA expression of paired samples was similar or independent. We compared differences in the expressions of paired and nonpaired CH and HCC samples using the Dunnett test¹² (Supplementary Data). All possible tests performed for data pairs represented no dependency due to the paired data from the same patients. For data analysis, we

used the standard pairwise class comparison and prediction tool in BRB ArrayTools.

Identification of Candidate miRNA Target Genes. Candidate target genes predicted to be regulated by miRNAs based on sequence comparison were selected using MIRANDA Pro3.0 (Sanger Institute). Of the selected genes, those represented on a microarray chip were then examined for expression (Fig. 4). The number of genes showing a significant ($P < 0.05$) expression difference among the candidate target genes represented on the chip was statistically analyzed to evaluate the significance of expression regulation by miRNAs. Analysis of significance was performed using Hotelling T2 test (BRB ArrayTools).

Pathway Analysis. Of the candidate miRNA target genes, those showing a significant ($P < 0.01$) expression difference between N, CH-B, HCC-B, CH-C, and HCC-C samples were analyzed for pathways involving these genes using MetaCore software suite (GeneGo, St. Joseph, MI). Significance probability was calculated using

Table 2-1. Class Prediction

No.	Class	Prediction (%)	No. of Predictors	P Value
1	HBV versus HCV	87	32	<0.001
2	N versus CH (B+C)	91	26	0.007
3	CH (B+C) versus HCC (B+C)	92	34	0.003

Class prediction algorithm was used for the classification of two groups of patients. Feature selection was based on the univariate significance level ($\alpha = 0.01$). The support vector machine classifier was used for class prediction.

Abbreviations: CH, nontumor lesion of HCC; HCC, hepatocellular carcinoma; N, normal.

Table 2-2 Binary Tree Classification

Node	Group 1 Class	Group 2 Class	No. of Predictors	Misclassification Rate (%)
1	HCC-B, HCC-C, CH-B, CH-C	N	20	4.9
2	HCC-B, CH-B	HCC-C, CH-C	19	13.5
3	HCC-B	CH-B	15	29.2
4	HCC-C	CH-C	14	17.9

Binary tree classification algorithm was used for the classification of each category of patients. Feature selection was based on the univariate significance level ($\alpha = 0.01$). The support vector machine classifier was used for class prediction. There were four nodes in the classification tree.

Abbreviations: CH-B, non-tumor lesion of HCC-B; CH-C, nontumor lesion of HCC-C; HCC-B, hepatitis B virus-related hepatocellular carcinoma; HCC-C, hepatitis C virus-related hepatocellular carcinoma; N, normal

Table 3-1. Representative miRNAs That Were Commonly Repressed in CH-B, CH-C, HCC-B, and HCC-C Compared with Normal Liver (Cluster)

miRNA	Parametric P Value	Ratio*	No. of Significant Genes/Predicted Target Genes†	Hotelling Test P Value‡	Differentially Expressed Target Genes§	Pathway of Regulated Genes¶
hsa-miR-219	7.3E-05	0.28	25/109	2.59E-04	Glypican-3, ERP5, PLK2, HIRA, HMG2 ACOX1 NF-X1	Regulatory T cell differentiation Fatty acid beta-oxidation MHC class II biosynthetic process
hsa-miR-320	9.8E-05	0.50	26/88	3.50E-06	Vimentin, ALP (N-acetyltransferase-like), SEC61 beta, G-protein alpha-i2, Filamin A Rac1, RhoG Vinexin beta, Profilin I, Ca-ATPase3	Protein kinase cascade Organelle organization and biogenesis Actin cytoskeleton organization and biogenesis
hsa-miR-154	2.7E-04	0.15	22/70	5.40E-06	OTR, NET1(TSPAN1), NAP1, Vimentin, PDIA3, cytochrome P-450 reductase DLX2 GUAC, ACAT1	Regulation of apoptosis Morphogenesis Branched chain family amino acid catabolic process
hsa-miR-29c	1.8E-03	0.55	53/133	1.00E-06	FBX07, ASPP1, HSPA4, Cathepsin O, PDF, COL4A1, HSPA4, TIP30, CXADR NS1-BP, ALP (N-acetyltransferase-like), ACTR10, Beclin 1 SMAD6, LTBR(TNFRSF3), ENPP7	Cell-substrate adhesion Transcription, DNA-dependent Apoptosis
hsa-miR-338	5.2E-03	0.46	30/101	3.60E-06	ID3, GATA-4, NFIA, FR-beta, CREST, HYOU1 G3ST1, CAD, FKBP12, LZIP, PDIA3, Schwannomin (NF2), CREST	Developmental process Immune effector process Immune system process
hsa-miR-26a	6.3E-03	0.70	37/119	2.64E-05	LIG4, c-FLIP, GADD45 beta, DAPK1, PRDX4, LRP130 Cyclin E, ZDHHC6, Tx1, ATG8 (GATE-16), WASP, C1s COPG1	Response to stimulus DNA replication initiation Ion transport
hsa-miR-126	8.1E-03	0.65	27/101	4.04E-03	ANP32B (april), HSPA4, RLI, LIV-1 (SLC39A6), PTP-MEG2, CD97, DHPR NFKBIA, NMI, MDH1, PDCD2 SMAD6, ATP6AP2, ANP32B (april), NMI, HSPA4	Regulation of cellular protein metabolic process Response to stress Apoptosis
hsa-miR-325	8.7E-03	0.20	18/63	2.03E-04	TRADD, CREST, NEDD8, annexin IV, GPX2, PDF, TNFAIP1 Glypican-3, ID1, PC-TP, SNRPB (Sm-B)	Developmental process Multicellular organismal development RNA splicing

*Ratio of HCC-B, HCC-C, CH-B, and CH-C to normal.

†The number of significant genes ($P < 0.05$) out of predicted target genes in which expression was evaluated in microarray.

‡Statistical assessment of presence of differentially expressed genes out of predicted target genes of miRNAs.

§Representative differentially expressed genes out of predicted target genes of miRNAs.

¶Representative pathway of differentially expressed genes out of predicted target genes of miRNAs.

the hypergeometrical distribution based on gene ontology terms. Because one gene is frequently involved in multiple pathways, all pathways corresponding to the genes with significance probability were listed.

Verification of Regulation of Candidate Target Genes by miRNAs. Anti-miRNA (Ambion) specific to 13 miRNAs (has-miR-17*, has-miR-20a, has-miR-23a, has-miR-26a, has-miR-27a, has-miR-29c, has-miR-30a, has-miR-92, has-miR-126, has-miR-139, has-miR-187, has-miR-200a, and has-miR-223) showing significant

differences in expression were transfected into Huh7 cells using TransMessenger transfection reagent (QIAGEN, Valencia, CA), and loss of function of each miRNA was evaluated. Similarly, precursor miRNAs of five miRNAs (has-miR-23a, has-miR-26a, has-miR-27a, has-miR-92, and has-miR-200a) were also transfected into Huh7 cells, and gain of function of each miRNA was evaluated. The loss- and gain-of-function of miRNAs were evaluated via RTD-PCR. In addition, different gene expressions regulated by miRNAs were also evaluated via RTD-PCR.

HBV/HCV Infection Model Using Cultured Cells.

The plasmid pHBV 1.2 coding the 1.2-fold length of the HBV genome was transfected into Huh7.5 cells using Fugene6 transfection reagent (Roche Applied Science, Indianapolis, IN). HBeAg production in culture medium was measured using Immunis HBeAg/Ab EIA (Institute of Immunology Co., Ltd., Tokyo, Japan).¹³ The amount of HBV-DNA was measured via RTD-PCR (Supplementary Fig. 1A,B). JFH1-RNA was transfected into Huh7.5 cells using TransMessenger transfection reagent (QIAGEN) and the expression of the core protein was examined via immunofluorescence staining using anti-HCV core antibody (Affinity BioReagent, CO).^{14,15} HCV-RNA amount was also measured via RTD-PCR (Supplementary Fig. 1A,B). JFH1/GND was used as a negative control. miRNA expression was quantitated by RTD-PCR 48 hours after transfection.

Results

Expression of miRNA in Liver Tissue. A panel of miRNA was successfully amplified from liver tissues via RTD-PCR. The representative amplification profile of miRNA as determined with RTD-PCR is shown in Fig. 1. To assess the reliability and reproducibility of this assay system, we first measured RNU6B in duplicate from all samples in different plates. The mean difference in Ct values of RNU6B expression within the same samples was 0.08 ± 0.05 (mean \pm standard deviation), indicating the high reproducibility of this assay. All Ct values from each reaction were collected, and Ct variation obtained by each probe from all patients was calculated. Although RNU6B was frequently used as the internal control, the standard Ct variation was relatively high (Ct, 27 ± 1.94), suggesting that the variances in its value depend on the state of liver disease (N, CH and HCC). Therefore, we selected has-miR-328 as the internal control with the smallest standard deviation (Ct, 30 ± 0.60). The relative expression ratio of individual miRNA to has-miR-328 was calculated and applied to the following analysis using a BRB-array tool.

Hierarchical cluster analysis revealed that the expression profiles of the 188 miRNAs from each patient were roughly classified into normal liver, HBV-infected liver (CH-B+HCC-B; HBV group), and HCV-infected liver (CH-C+HCC-C; HCV group) (Fig. 2A). HCV viremia in two patients with CH-C was persistently cleared by interferon therapy before HCC development. The background liver of one of these patients was clustered in the normal group and those of others in the HCV group. Although these two patients were not clearly differentiated from others, some miRNAs such as miR-194, miR-

211, and miR-340 that were down-regulated in the HCV group were significantly up-regulated in two patients (Fig. 3, cluster 2).

The present CH and HCC expression data were obtained from the same patient; however, each sample clustered irrespective of pairs in all but two patients. miRNA expression profiling was therefore more dependent on the disease condition than on the paired condition, as also confirmed by the Dunnett test.¹² We then attempted to classify the expression profiles into HBV and HCV groups using supervised learning methods (Table 2-1). HBV and HCV groups were significantly differentiated at an 87% accuracy ($P < 0.001$). The normal liver and CH (CH-B + CH-C) and CH and HCC (HCC-B + HCC-C) were also significantly differentiated at a 90% rate of accuracy. These results suggest that different stages of liver disease (normal, CH, and HCC) can be differentiated from each other based on the miRNA expression profile, as well as HBV and HCV infection.

To examine the relationship among five categories of groups, namely, N, CH-B, CH-C, HCC-B and HCC-C, we attempted to differentiate the five groups using a supervised learning algorithm (binary tree classification) used for classifying three or more groups. SVM was used as a prediction method. Expression profiles were first classified into groups N (normal) and non-N (non-normal) (CH-C, CH-B, HCC-C, and HCC-B) (node 1) ($P < 0.01$). The non-N group was then classified into HBV and HCV (node 2) ($P < 0.01$). The HBV group was further classified into CH-B and HCC-B (node 3) ($P < 0.01$), and the HCV group was further classified into CH-C and HCC-C (node 4) ($P < 0.01$) (Fig. 2B, Table 2-2). Thus, the findings support the notion that differences in miRNA expression between HBV and HCV are as distinct as those between CH and HCC.

Out of 20 miRNAs that differentiated node 1 classification (Table 2-2), 12 also differentiated node 3 or node 4 classification. The remaining eight miRNAs specifically differentiated node 1 classification. They were down-regulated in the HBV and HCV groups compared with the normal group (Fig. 3, cluster 1). Nineteen miRNAs differentiated node 2 classification (Table 2-2) and the hierarchical clustering using these miRNAs clearly differentiated the HBV and HCV groups (Fig. 3, cluster 2). There were 15 and 14 miRNAs that differentiated node 3 and 4 classifications, respectively (Table 2-2). Hierarchical clustering using these miRNAs revealed that these miRNAs differentiated CH-B and HCC-B as well as CH-C and HCC-C, respectively; 17 miRNAs were down-regulated in HCC, and six were up-regulated in HCC (Fig. 3, cluster 3).

Table 3-2. Differentially Expressed miRNA Between HCC-B, CH-B, and HCC-C, CH-C, and Their Representative Target Genes (Cluster 2)

miRNA	Parametric P Value	Ratio*	No. of Significant Genes/Predicted Target Genes†	Hotelling Test P Value‡	Differentially Expressed Target Genes§	Pathway of Regulated Genes¶
hsa-miR-190	1.2E-05	2.06	21/68	4.47E-02	Chk1, C2orf25, VRK2, USP16, STAF65(gamma) AP1S2, RNASE4	Regulation of cell cycle Mitotic cell cycle
hsa-miR-134	2.3E-04	5.74	11/58	3.40E-06	PPP2R1B, ARHGAP15, UBPY VKDGC, SH2B, MALS-1, DDB2 BCRP1 DDB2	Negative regulation of apoptosis Multicellular organismal process Regulation of viral reproduction Lipid biosynthetic process
hsa-miR-151	2.8E-04	1.82	12/62	6.41E-01	RGS2, UFO, AK2, USP7 eIF4G2, USP7 SLC22A7	G-protein signaling Regulation of translation Organic anion transport
hsa-miR-193	5.0E-04	1.67	23/95	9.30E-01	G-protein alpha-11, p130CAS, VAV-1, PDCD11 Colipase, ACSA DCOR	Cell motility Energy coupled proton transport Intracellular signaling cascade
hsa-miR-133b	1.7E-03	2.42	20/97	3.69E-02	DDB2, Bcl-3, Cystatin B Rab-3, RAG1AP1, KCNH2, DCOR AL1B1	Proteasomal protein catabolic process Regulation of biological quality Carbohydrate metabolic process
hsa-miR-324-5p	2.9E-03	1.51	27/121	1.90E-06	SKAP55, VAV-1, DDB2, E2A, NIP1 MEMO (CGI-27), Rab-3 COPG1, GPX3, OAZ2	Cellular developmental process Cellular structure morphogenesis Glutathione metabolic process
hsa-miR-182*	3.1E-03	2.23	28/123	< 1e-07	Alpha-endosulfine, HCCR-2, Thioredoxin-like 2, TPT1, USP7 DDB2, TPT1 JIP-1	Translation initiation in response to stress Cellular developmental process JNK cascade
hsa-miR-105	4.6E-03	4.38	18/68	4.74E-05	Beta-2-microglobulin, HLA-B27 PIMT, IL-17RC MHC class I, CDK9, ERG1, Desmocollin 3 PSMD5, SLC26A6	Antigen processing and presentation Immune response Proteasomal protein catabolic process
hsa-miR-211	5.3E-03	25.61	10/56	2.00E-04		Regulation of apoptosis
hsa-miR-20	5.7E-03	1.52	27/113	5.28E-03	Noelin, SC4MOL, Thioredoxin-like 2, CCL5, NALP3 Hic-5/ARA55, USP16, MAP4, Ferroportin 1	Positive regulation of cellular process Oxygen transport
hsa-miR-191	6.7E-03	1.39	25/79	7.55E-04	TOP3A, PLRP1 CDK9, GPS2, CLTA, LXR-alpha ACSA UGCG11, SGPP1	Nucleic acid metabolic process Acetyl-CoA biosynthetic process Metal ion transport
hsa-miR-340	8.5E-03	1.48	17/81	3.73E-03	FKBP12, DCOR, Gelsolin, VAV-1, ARF6	Calcium ion transport Actin cytoskeleton organization and biogenesis
hsa-miR-194	8.7E-03	1.67	13/74	5.90E-01	HXK3 Cyclin B1, Serglycin PTE2 SLC7A6	Glucose catabolic process M phase of mitotic cell cycle Acyl-CoA metabolic process Carbohydrate utilization
hsa-miR-23a	1.9E-04	0.46	14/97	< 1e-07	RGL2, MANR, MEK1 (MAP2K1), Caspase-3, AZGP1 FRK, Pyk2(FAK2), CSE1L AZGP1	Protein kinase cascade Cellular developmental process Defense response
hsa-miR-142-5p	4.9E-04	0.40	25/89	9.10E-06	Sirtuin4, PAI2, PSAT, RIL, CDC34, SPRY1 E4BP4, DNAJC12, WWP1, PAIP1, PASK, rBAT VCAM1, CaMK I, WWP1, FHL3	Metabotropic glutamate receptor Regulation of gene expression Cell-matrix adhesion
hsa-miR-34c	5.1E-04	0.20	31/129	7.30E-06	Diacylglycerol kinase, zeta, PLC-delta 1, ATP2C1, PAI2 MLK3(MAP3K11), MEK1(MAP2K1), CDC25C, MRF-1, XPC GNT-IV	Manganese ion transport Protein kinase cascade Inflammatory cell apoptosis

Table 3-2. Continued

miRNA	Parametric P Value	Ratio*	No. of Significant Genes/Predicted Target Genes†	Hotelling Test P Value‡	Differentially Expressed Target Genes§	Pathway of Regulated Genes¶
hsa-miR-124b	8.6E-04	0.32	25/120	7.10E-05	E2F5, Rad51, Jagged1 MLK3(MAP3K11), RGS1 COL16A1	Muscle development Intracellular signaling cascade MAPKKK cascade
hsa-let-7a	1.0E-03	0.45	28/136	9.35E-04	RAD51C, CoAA, hASH1, Cockayne syndrome B, Caspase-1, PP5 PLC-delta 1, MANR, ACADVL HGF, NGF	Response to DNA damage stimulus Fibroblast proliferation Cellular developmental process
hsa-miR-27a	3.9E-03	0.59	18/108	1.19E-02	COL16A1, RIL, RhoGDI gamma, ANP32B (april) VE-cadherin, NTH1, GATA-2, E4BP4 RAD51C	Cytoskeleton organization and biogenesis Response to external stimulus DNA recombination

*Ratio of HCC-B, CH-B, to HCC-C,CH-C.

†The number of significant genes ($p < 0.05$) out of predicted target genes in which expression was evaluated in microarray.

‡Statistical assessment of presence of differentially expressed genes out of predicted target genes of miRNAs.

§Representative differentially expressed genes out of predicted target genes of miRNAs.

¶Representative pathway of differentially expressed genes out of predicted target genes of miRNAs.

These results indicate that there were two types of miRNAs—one associated with HBV and HCV infection (cluster 2), the other associated with the stages of liver disease (clusters 1 and 2) that were irrelevant to the differences in HBV and HCV infection.

Differential miRNAs and Their Candidate Target Genes and Signaling Pathways. Differentially expressed miRNAs are shown in Table 3. In addition to the expression ratios of miRNAs in each group, the number of genes analyzed on the microarray predicted to be the target genes of miRNAs and that which actually showed significant ($P < 0.05$) differences in expression are also shown. Based on the frequencies and levels of expression of differential genes, the significance of regulation of these gene groups by miRNAs was evaluated using Hotelling T2 test (BRB ArrayTools) (Table 3). The representative candidate target genes and their signaling pathways by each miRNA were shown one by one (Table 3). The signaling pathways regulated by all differential miRNAs in each category of groups are shown in Table 4.

Eight miRNAs were down-regulated in the HBV and HCV groups compared with the normal group (Table 3-1; Fig. 3, cluster 1). These miRNAs were associated with an increased expression of genes related to cell adhesion, cell cycle, protein folding, and apoptosis (Tables 3-1, 4-1), and possibly with the common feature of CH irrespective of the differences in HBV and HCV infection.

Nineteen miRNAs clearly differentiated the HBV and HCV groups (Fig. 3, cluster 2, Table 3-2). Thirteen miRNAs exhibited a decreased expression in the HCV group, and six showed a decreased expression in the HBV group. miRNAs exhibiting a decreased expression in the HCV group regulate genes related to immune response,

antigen presentation, cell cycle, proteasome, and lipid metabolism. On the other hand, those exhibiting a decreased expression in the HBV group regulate genes related to cell death, DNA damage and recombination, and transcription signals. These findings reflected the differences in the gene expression profile between CH-B and CH-C described (Tables 3-2, 4-2).¹⁰ Interestingly, although these miRNAs were HBV and HCV infection-specific, some of them were reported to be tumor-associated miRNAs, suggesting the possible involvement of infection-associated miRNAs in HCC development.

Twenty-three miRNAs clearly differentiated CH and HCC that were irrelevant to the differences in HBV and HCV infection. Seventeen miRNAs were down-regulated in HCC that up-regulated cancer-associated pathways such as cell cycle, adhesion, proteolysis, transcription, translation, and the Wnt signaling pathway (Tables 3-3, 4-3). Six miRNAs were up-regulated in HCC that down-regulated all inflammation-mediated signaling pathways, potentially reflecting impaired antitumor immune response.

Relationship Between Expressions of Infection-Associated miRNA in Liver and Cultured Cells Infected with HBV and HCV. To clarify whether the expression of infection-associated miRNA is regulated by HBV and HCV infection, we investigated the relationship between changes in miRNA in liver tissues and those in miRNA in Huh7.5 cells in which infectious HBV or HCV clones replicated. To evaluate the replication of each clones in Huh7.5 cells, we measured time-course changes in the amounts of HBV-DNA and HCV-RNA in Huh7.5 cells transfected with pHBV1.2 and JFH1-RNA, respectively, by RTD-PCR (Supplementary Fig. 1A). The expression of HBV proteins was examined by measuring the amount

Table 3-3. Differentially Expressed miRNA Between CH and HCC and Their Representative Target Genes (Cluster 3)

miRNA	Parametric p-value	Ratio*	No. of Significant Genes/Predicted Target Genes†	Hotelling Test P Value‡	Differentially Expressed Target Genes§	Pathway of Regulated Genes¶
hsa-miR-139	4.50E-06	0.42	19/106	2.70E-03	Cyclin B1, DHX15, MCM5, Histone H2A RBCK1, SYHH	Mitotic cell cycle Protein catabolic process
hsa-miR-30a-3p	2.50E-05	0.49	26/144	1.73E-02	ILK, IGFBP7, SAFB, CTR9 GGH, Pirin, ZNF207, Annexin VII ILK, LTA4H, ABC50, GNPAT	Response to external stimulus Regulation of oxidoreductase activity Cell-matrix adhesion
hsa-miR-130a	7.00E-05	0.50	22/108	1.07E-02	DLC1 SPHM, PPP2R5D, RHEB2, SPHM MLK3(MAP3K11), Otubain1, TIMP4 NRBP	Morphogenesis Mitotic cell cycle Protein modification process Cell differentiation
hsa-miR-223	3.40E-04	0.39	14/90	6.52E-03	Ephrin-A1, Midkine, FDPS K(+) channel, subfamily J	Cell morphogenesis Notch signaling pathway
hsa-miR-187	3.55E-04	0.12	16/66	6.76E-04	HFE2, Otubain1	Negative regulation of programmed cell death
hsa-miR-200a	6.86E-04	0.18	20/141	2.15E-02	PRSS11, SUPT5H, RAG1AP1 PLOC3 CDC25B, KAP3, CDK2AP2, CHKA POLD CPSF4	Developmental process Mitochondrial ornithine transport Cell communication DNA replication RNA splicing
hsa-miR-17-3p	8.42E-04	0.58	28/108	8.98E-04	MLK3(MAP3K11), Tip60, ACBD6, DOC-1R, DAX1, RBCK1 WNT5A, 14-3-3 gamma, DHX15 HFE2, MCM5	Protein kinase cascade BMP signaling pathway DNA recombination
hsa-miR-99a	1.17E-03	0.53	33/163	9.52E-03	Calpain small subunit, Thoredoxin-like 2, Survivin IBP2, DNA-PK, KAP3, NFE2L1, PARP-1, HDAC11	Cytokinesis Intracellular signaling cascade Regulatory T cell differentiation
hsa-miR-200b	1.57E-03	0.18	24/147	2.72E-02	HSP47, HMG2, NRBP SNX17	Regulation of cell cycle Cell motility
hsa-miR-125b	1.82E-03	0.55	26/114	1.03E-01	Ephrin-A1 COL4A2, TIP30, HSP47, MSP58 MLK3(MAP3K11), ERK2 (MAPK1), ERK1 (MAPK3), PLOC3 Otubain1, SCN4A(SKM1)	Receptor protein signaling pathway Cell adhesion Nuclear translocation of MAPK Ubiquitin-dependent protein catabolic process
hsa-miR-30e	2.10E-03	0.65	24/151	4.30E-02	Cyclin B1, XTP3B, GAK, Annexin VII, MIC2, NRBP MSS4 S100A10	Mitotic cell cycle Protein localization Calcium ion transport
hsa-miR-199a*	4.26E-03	0.35	11/71	7.16E-02	BUB3, Cyclin B1, LMNBR PRAME	Mitotic cell cycle Cardiac muscle cell differentiation
hsa-miR-122a	6.31E-03	0.51	11/80	1.01E-03	JAB1, APEX, Clathrin heavy chain PARN DDAH2	Base-excision repair Translational initiation Regulation of cellular respiration
hsa-miR-199a	8.77E-03	0.35	18/94	3.56E-02	IL-13, MLK3(MAP3K11), CLK2, ACP33 PAFAH beta, SPA1, CLCN4	Protein amino acid phosphorylation Small GTPase mediated signal transduction
hsa-miR-326	9.00E-03	0.57	29/147	2.25E-01	Midkine, ENT1, IP3KA, PSMC5, ANCO-1 Thy-1, MCM6, Tip60, VILIP3 COMP, Cathepsin A	Regulation of programmed cell death Cell-matrix adhesion Blood vessel development
hsa-miR-92	9.60E-03	0.81	28/140	2.47E-02	TUBGCP2, Fibrillin 1, PIPKI gamma, KAP3 SNX15, BCAT2 IGFBP7, FZD6, COPS6	Rho protein signal transduction LDL receptor and BCAA metabolism Adenosine receptor signaling pathway
hsa-miR-221	3.40E-06	3.34	16/67	3.59E-01	Lck, Kallistatin, Neuromodulin, LFA-3, PA24A, AZGP1, MSH2 KYNU, PMCA3	Immune response-activating signal transduction DNA repair

Table 3-3. Continued

miRNA	Parametric p-value	Ratio*	No. of Significant Genes/Predicted Target Genes†	Hotelling Test P Value‡	Differentially Expressed Target Genes§	Pathway of Regulated Genes¶
hsa-miR-222	6.50E-06	2.23	18/85	1.59E-02	Thrombospondin 1, Lck, MSH2, ATF-2, CITED2, Kallistatin	Cell motility
hsa-miR-301	5.22E-05	1.96	14/71	1.16E-01	PGAR KYN Beta-2-microglobulin, PPCKM, PRC, Fra-1, PPCKM, ACAT2	Triacylglycerol metabolic process DNA replication Antigen processing and presentation
hsa-miR-21	7.67E-03	1.57	19/81	1.86E-04	BMPR1B, ARMER, EHM2, RBBP8 Neuromodulin, LDLR	Meiotic recombination Cell motility
hsa-miR-183	2.46E-02	3.51	13/86	3.36E-01	Btk, Fra-1, MSH2, Collectrin, Adipophilin	Regulation of T cell proliferation
hsa-miR-98	5.22E-02	1.32	24/130	2.95E-04	RNASE4, AGXT2L1 SARDH	Peptidyl-tyrosine phosphorylation Natural killer cell activation during immune response
					Hdj-2, PEMT, Lck, MKP-5, Chondromodulin-1, ABCA8	Cell differentiation
					IL-16, MTRR, SerRS	Methionine biosynthetic process
					ACAA2, LTB4DH, ACADVL, DECR, S14 protein,	Fatty acid metabolic process
					Rapsyn, Kallistatin, ENPEP, Beta crystallin B1	Multicellular organismal process
					CYP4F8	Prostaglandin metabolic process

*Ratio of HCC to CH.

†The number of significant genes ($P < 0.05$) out of predicted target genes in which expression was evaluated in microarray.

‡Statistical assessment of presence of differentially expressed genes out of predicted target genes of miRNAs.

§Representative differentially expressed genes out of predicted target genes of miRNAs.

¶Representative pathway of differentially expressed genes out of predicted target genes of miRNAs.

of HBeAg released in culture medium (Supplementary Fig. 1B). HCV protein expression was examined by evaluating the core protein expression after 48 hours by fluorescence immunostaining (Supplementary Fig. 1C). RNA was extracted from the Huh7.5 cells 48 hours after gene transfection, and miRNA expression pattern in the cells was compared with those in liver tissues. We found a strong correlation between differences in miRNA expression between liver tissues of the HBV and HCV groups, and those in miRNA expression between Huh7.5 cells transfected with HBV and HCV clones ($r = 0.73$, $P = 0.0006$) (Fig. 5). These results revealed that differences in the expression of infection-associated miRNA in the liver between the HBV and HCV groups are explained by changes in miRNA expression caused by HBV and HCV infections.

Verification of Regulation of Candidate Target Genes by miRNA. Anti-miRNAs (Ambion) specific to 13 miRNAs (has-miR-17*, has-miR-20a, has-miR-23a, has-miR-26a, has-miR-27a, has-miR-29c, has-miR-30a, has-miR-92, has-miR-126, has-miR-139, has-miR-187, has-miR-200a, and has-miR-223) showing significant differences in expression were transfected into Huh7 cells to examine loss of function of the miRNAs. Five miRNAs (has-miR-23a, has-miR-26a, has-miR-27a, has-miR-92, and has-miR-200a) showed a decreased expression by

more than 50%. Precursor miRNAs of these miRNAs were also transfected into the cells to examine the gain of function of the miRNAs (Supplementary Fig. 2). It was confirmed that the expressions of target genes of the five miRNAs (LIG4 [by has-miR-26a]; RGL2 [by has-miR-23a]; Rad51C [by has-miR-27a]; KAP3, CDC25B, KAP3, CDK2AP2, POLD, and CPSF4 [by has-miR-200a]; and TUBGCP2, SNX15 and BCAT2 [by has-miR-92]) were increased by the suppression of the miRNAs induced by anti-miRNAs and were decreased by the overexpression of precursor miRNAs (Supplementary Fig. 3).

Discussion

miRNA plays an important role in various diseases such as infection and cancer.¹⁻³ In this study, we examined miRNA expression profiles in normal liver and HCC, including nontumor lesions infected with HBV or HCV. Although the expression profiles of miRNAs in HCC have been reported,¹⁶⁻¹⁸ most of the studies were performed using a microarray system. Because we thought that miRNAs could not produce enough detection signals owing to their short length, we applied a highly sensitive and quantitative RTD-PCR method for miRNAs. Moreover, global gene expression in the same tissues was ana-

Table 4-1. Pathway Analysis of Targeted Genes by miRNAs that Were Commonly Repressed in CH-B, CH-C, HCC-B, and HCC-C Compared with Normal Liver (Cluster 1)

No.	Pathway Name	P Value
Down-regulated miRNA in CH-B,HCC-B,CH-C and HCC-C (possibly up-regulating target genes)		
1	Cell adhesion_Platelet-endothelium-leukocyte interactions	1.11E-02
2	Cell cycle_S phase	2.18E-02
3	Protein folding_Protein folding nucleus	2.43E-02
4	Cell cycle_G1-S	3.07E-02
5	Development_Cartilage development	3.89E-02
6	Protein folding_Folding in normal condition	3.89E-02
7	Proteolysis_Connective tissue degradation	3.99E-02
8	Proteolysis_Proteolysis in cell cycle and apoptosis	4.31E-02
9	Signal Transduction_BMP and GDF signaling	5.81E-02
10	Immune_Antigen presentation	6.05E-02

lyzed via cDNA microarray to examine whether the differentially expressed miRNAs could regulate their target genes. Because the absolute standard of miRNA is not available at present, and miRNA expression was compared within the samples and genes analyzed in this study, there might be possible errors when a larger number of samples and genes were analyzed.

Using these systems, we found that the expression profile in miRNAs was clearly different according to HBV and HCV infection for the first time. The differences were confirmed by the nonsupervised learning method, hierar-

Table 4-2. Pathway Analysis of Targeted Genes by Differentially Expressed miRNAs Between HBV-Related Liver Disease (CH-B,HCC-B) and HCV Related Liver Disease (CH-C,HCC-C Cluster 2)

No.	Pathway Name	P Value
Down-regulated miRNA in CH-C,HCC-C (possibly up-regulating target genes)		
1	Immune_Phagosome in antigen presentation	5.80E-04
2	Muscle contraction	1.05E-03
3	Immune_Antigen presentation	5.75E-03
4	Cell cycle_Meiosis	1.49E-02
5	Reproduction_Male sex differentiation	2.06E-02
6	Cell adhesion_Platelet aggregation	2.77E-02
7	Transport_Synaptic vesicle exocytosis	3.56E-02
8	Inflammation_Kallikrein-kinin system	3.73E-02
9	Inflammation_IgE signaling	4.10E-02
10	Development_Skeletal muscle development	5.02E-02
Down-regulated miRNA in CH-B,HCC-B (possibly up-regulating target genes)		
1	Signal Transduction_Cholecystokinin signaling	1.15E-04
2	Inflammation_NK cell cytotoxicity	5.29E-03
3	Signal transduction_CREM pathway	5.31E-03
4	Reproduction_GnRH signaling pathway	7.80E-03
5	DNA damage_DBS repair	1.02E-02
6	Cell cycle_G2-M	1.63E-02
7	Development_Neuromuscular junction	2.07E-02
8	Apoptosis_Apoptosis mediated by external signals	2.42E-02
9	Reproduction_FSH-beta signaling pathway	2.92E-02
10	Cell adhesion_Amyloid proteins	3.81E-02

Table 4-3. The Pathway Analysis of Targeted Genes by Differentially Expressed miRNAs Between CH and HCC (Cluster 3)

No.	Pathway Name	P Value
Down-regulated miRNA in HCC (possibly up-regulating target genes)		
1	Cytoskeleton_Spindle microtubules	2.15E-03
2	Transcription_Chromatin modification	5.27E-03
3	Proteolysis_Ubiquitin-proteasomal proteolysis	6.43E-03
4	Cell adhesion_Cell-matrix interactions	7.30E-03
5	Cell cycle_Meiosis	7.83E-03
6	DNA damage_Checkpoint	1.69E-02
7	Reproduction_Progesterone signaling	1.94E-02
8	Apoptosis_Apoptotic mitochondria	3.14E-02
9	Translation_Regulation of initiation	4.22E-02
10	Signal transduction_WNT signaling	4.26E-02
Up-regulated miRNA in HCC (possibly down-regulating target genes)		
1	Inflammation_IgE signaling	1.05E-02
2	Inflammation_Kallikrein-kinin system	2.46E-02
3	Inflammation_Innate inflammatory response	2.51E-02
4	Inflammation_Histamine signaling	4.25E-02
5	Inflammation_Neutrophil activation	4.55E-02
6	Chemotaxis	4.68E-02
7	Inflammation_IL-12,15,18 signaling	5.16E-02
8	Inflammation_NK cell cytotoxicity	7.25E-02
9	Cell cycle_G0-G1	7.53E-02
10	Inflammation_Complement system	7.72E-02

chical clustering (Fig. 2A), and supervised learning methods based on SVM at an 87% accuracy ($P < 0.001$) (Table 2-1). As similarly described, the expression profile in miRNAs was significantly different according to the progression of liver disease (normal, CH, and HCC) in this study. The present CH and HCC expression data were derived from the same patient, and some microarray analyses suggested that the noncancerous liver tissue can predict the prognosis of HCC.^{19,20} We examined whether the miRNA expression of paired samples was similar or independent using the Dunnett test¹² (Supplementary Data). Our data indicated that miRNA expression profiling was more dependent on the disease condition than on the paired condition, although the issue of paired samples should be taken into account carefully.

Binary tree prediction analysis and detailed assessment of hierarchical clustering revealed two types of differential miRNAs, one associated with HBV and HCV infection, the other associated with the stages of liver disease that were irrelevant to the differences in HBV and HCV infection. We found that differences in miRNA expression between liver tissues with HBV and HCV (HBV/HCV) were strongly correlated with those in miRNA between cultured cell models of HBV and HCV infection (HBV/HCV) ($r = 0.73$ $P = 0.0006$) (Fig. 5). Thus, there exist HBV- and HCV-infection-specific miRNAs that potentially regulate viral replication and host gene signaling pathways in hepatocytes.

	HBV/HCV	
	Tissue	Huh7.5
hsa-miR-20	0.61	0.36
hsa-miR-23a	-1.12	-1.3
hsa-miR-27a	-0.75	-1.51
hsa-miR-34c	-2.29	N.D.
hsa-miR-105	2.13	N.D.
hsa-miR-124b	-1.63	-10.54
hsa-miR-133b	1.28	-3.64
hsa-miR-134	2.52	-0.63
hsa-miR-142-5p	-1.34	-4.39
hsa-miR-151	0.86	-0.29
hsa-miR-182*	1.16	0.37
hsa-miR-190	1.04	1.32
hsa-miR-191	0.48	1.16
hsa-miR-193	0.74	-0.03
hsa-miR-194	0.74	0.76
hsa-miR-211	4.68	5.26
hsa-miR-324-5p	0.59	1.16
hsa-miR-340	0.57	1.68
hsa-let-7a	-1.14	-4.51

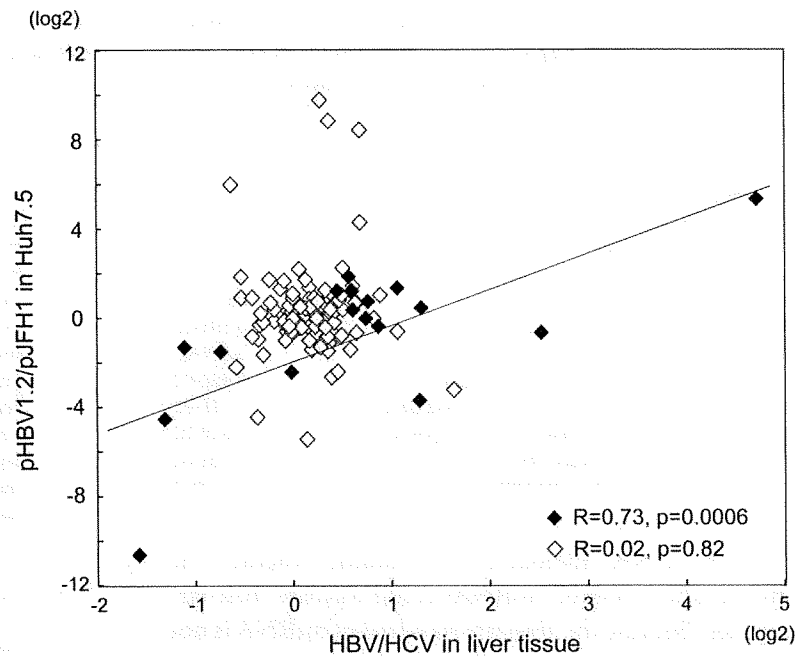


Fig. 5. Correlation between differences in miRNA expression between liver tissues infected with HBV and HCV and those in miRNA expression between cultured cell models of HBV and HCV infections. A total of 140 of 188 miRNAs were confirmed to be expressed in Huh7.5 cells. There was a significant correlation of infection-associated miRNA (closed lozenge) in vitro and in vivo ($r = 0.73$, $P = 0.0006$), but none for the other 121 miRNAs (open lozenge) ($r = 0.02$, $P = 0.82$).

The pathway analysis of targeted genes by miRNAs revealed that 13 miRNAs exhibiting a decreased expression in the HCV group regulate genes related to immune response, antigen presentation, cell cycle, proteasome, and lipid metabolism. Six miRNAs showing a decreased expression in the HBV group regulate genes related to cell death, DNA damage and recombination, and transcription signals. These findings reflected differences in the gene expression profile between CH-B and CH-C as described.¹⁰ Many of the miRNAs were down-regulated in the HCV group rather than in the HBV group. It has been reported that human endogenous miRNAs may be involved in defense mechanisms, mainly against RNA viruses.²¹ On the other hand, it is suggested that endogenous miRNAs may be consumed and reduced by defense mechanisms, especially those against RNA viruses.

Although the expressions of these HBV- and HCV-infection-specific miRNAs were irrelevant to the differences in CH and HCC (Fig. 3, cluster 2), some of them have been reported to play pivotal roles in the occurrence of cancer. For example, has-let-7a regulates ras and c-myc genes,²² and has-miR-34 is involved in the p53 tumor suppressor pathway.²³ These miRNAs were down-regulated in the HBV group, possibly participating in a more aggressive and malignant phenotype in HCC-B rather than in HCC-C. High expression of has-miR-191 was shown to be significantly associated with the worse survival in acute myeloid leukemia,²⁴ and has-miR-191 was

overexpressed in the HBV group compared with the HCV group. On the other hand, has-miR-133b, which was reported to be down-regulated in squamous cell carcinoma,²⁵ was repressed in the HCV group compared with the HBV group. Some hematopoietic-specific miRNAs such as has-miR-142-5p were up-regulated in the HCV group. Therefore, these miRNAs were not only HBV and HCV infection-associated but also tumor-associated. These findings indicate different mechanisms of development of HCC infected with HBV and HCV (Fig. 6).

Following HCC development, common changes in miRNA expression between HCC-B and HCC-C appeared (Fig. 3, cluster 3). The 23 miRNAs mentioned above clearly differentiated CH and HCC that were irrelevant to the differences in HBV and HCV infections. Seventeen miRNAs were down-regulated in HCC, which up-regulated cancer-associated pathways. Six miRNAs were up-regulated in HCC that down-regulated all inflammation-mediated signaling pathways, potentially reflecting impaired antitumor immune response in HCC. These results suggest that common signaling pathways are involved in HCC development from CH, and that HBV- and HCV-specific miRNAs participate in generating HCC-specific miRNA expressions (Fig. 6). Therefore, these miRNAs might be good candidates for molecular targeting to prevent HCC occurrence, because they reg-

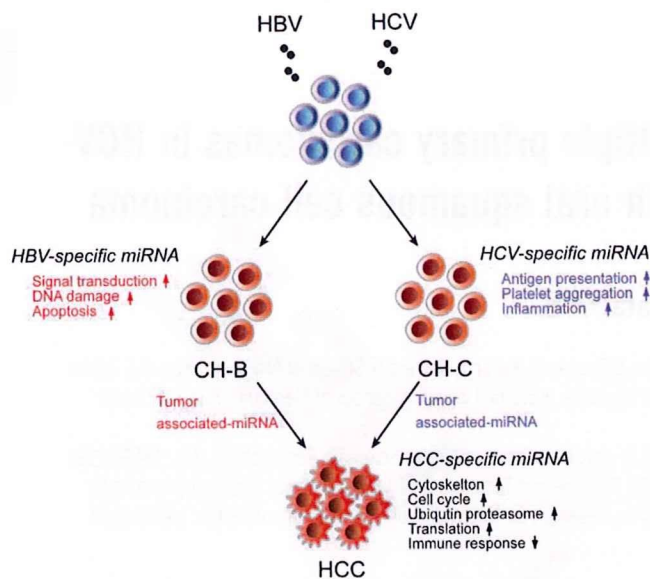


Fig. 6. Infection-associated and HCC-specific miRNAs and liver disease progression.

ulate a common signaling pathway underlying HCC-B and HCC-C development.

In conclusion, we showed that miRNAs are important mediators of HBV and HCV infections as well as liver disease progression. Further studies are needed to enable more detailed mechanistic analysis of the miRNAs identified here and to evaluate the usefulness of miRNAs as diagnostic/prognostic markers and potential therapeutic target molecules.

Acknowledgement: The authors thank Mikiko Nakamura and Nami Nishiyama for excellent technical assistance.

References

- He L, Thomson JM, Hemann MT, Hernando-Monge E, Mu D, Goodson S, et al. A microRNA polycistron as a potential human oncogene. *Nature* 2005;435:828-833.
- Calin GA, Dumitru CD, Shimizu M, Bichi R, Zupo S, Noch E, et al. Frequent deletions and down-regulation of micro-RNA genes miR15 and miR16 at 13q14 in chronic lymphocytic leukemia. *Proc Natl Acad Sci U S A* 2002;99:15524-15529.
- Cho WC. OncomiRs: the discovery and progress of microRNAs in cancers. *Mol Cancer* 2007;6:60.
- Hutvagner G, Zamore PD. A microRNA in a multiple-turnover RNAi enzyme complex. *Science* 2002;297:2056-2060.
- Ambros V, Bartel B, Bartel DP, Burge CB, Carrington JC, Chen X, et al. A uniform system for microRNA annotation. *RNA* 2003;9:277-279.
- Lee RC, Feinbaum RL, Ambros V. The *C. elegans* heterochronic gene *lin-4* encodes small RNAs with antisense complementarity to *lin-14*. *Cell* 1993;75:843-854.
- Lewis BP, Burge CB, Bartel DP. Conserved seed pairing, often flanked by adenosines, indicates that thousands of human genes are microRNA targets. *Cell* 2005;120:15-20.
- Kiyosawa K, Sodeyama T, Tanaka E, Gibo Y, Yoshizawa K, Nakano Y, et al. Interrelationship of blood transfusion, non-A, non-B hepatitis and hepatocellular carcinoma: analysis by detection of antibody to hepatitis C virus. *HEPATOLOGY* 1990;12:671-675.
- Honda M, Kaneko S, Kawai H, Shirota Y, Kobayashi K. Differential gene expression between chronic hepatitis B and C hepatic lesion. *Gastroenterology* 2001;120:955-966.
- Honda M, Yamashita T, Ueda T, Takatori H, Nishino R, Kaneko S. Different signaling pathways in the livers of patients with chronic hepatitis B or chronic hepatitis C. *HEPATOLOGY* 2006;44:1122-1138.
- Molinari AM, Simon R, Pfeiffer RM. Prediction error estimation: a comparison of resampling methods. *Bioinformatics* 2005;21:3301-3307.
- Dunnnett CW. A multiple comparison procedure for comparing several treatments with a control. *J Am Stat Assoc* 1955;50:1096-1121.
- Weiss L, Kekule AS, Jakubowski U, Burgelt E, Hofschneider PH. The HBV-producing cell line HepG2-4A5: a new in vitro system for studying the regulation of HBV replication and for screening anti-hepatitis B virus drugs. *Virology* 1996;216:214-218.
- Lindenbach BD, Evans MJ, Syder AJ, Wolk B, Tellinghuisen TL, Liu CC, et al. Complete replication of hepatitis C virus in cell culture. *Science* 2005;309:623-626.
- Wakita T, Pietschmann T, Kato T, Date T, Miyamoto M, Zhao Z, et al. Production of infectious hepatitis C virus in tissue culture from a cloned viral genome. *Nat Med* 2005;11:791-796.
- Murakami Y, Yasuda T, Saigo K, Urashima T, Toyoda H, Okanoue T, et al. Comprehensive analysis of microRNA expression patterns in hepatocellular carcinoma and non-tumorous tissues. *Oncogene* 2006;25:2537-2545.
- Varnholt H, Dreber U, Schulze F, Wedemeyer I, Schirmacher P, Dienes HP, et al. MicroRNA gene expression profile of hepatitis C virus-associated hepatocellular carcinoma. *HEPATOLOGY* 2008;47:1223-1232.
- Budhu A, Jia HL, Forgues M, Liu CG, Goldstein D, Lam A, et al. Identification of metastasis-related microRNAs in hepatocellular carcinoma. *HEPATOLOGY* 2008;47:897-907.
- Budhu A, Forgues M, Ye QH, Jia HL, He P, Zanetti KA, et al. Prediction of venous metastases, recurrence, and prognosis in hepatocellular carcinoma based on a unique immune response signature of the liver microenvironment. *Cancer Cell* 2006;10:99-111.
- Hoshida Y, Villanueva A, Kobayashi M, Peix J, Chiang DY, Camargo A, et al. Gene expression in fixed tissues and outcome in hepatocellular carcinoma. *N Engl J Med* 2008;359:1995-2004.
- Jopling CL, Yi M, Lancaster AM, Lemon SM, Sarnow P. Modulation of hepatitis C virus RNA abundance by a liver-specific MicroRNA. *Science* 2005;309:1577-1581.
- Johnson CD, Esquela-Kerscher A, Stefani G, Byrom M, Kelnar K, Ovcharenko D, et al. The let-7 microRNA represses cell proliferation pathways in human cells. *Cancer Res* 2007;67:7713-7722.
- He X, He L, Hannon GJ. The guardian's little helper: microRNAs in the p53 tumor suppressor network. *Cancer Res* 2007;67:11099-11101.
- Garzon R, Volinia S, Liu CG, Fernandez-Cymering C, Palumbo T, Pichiorri F, et al. MicroRNA signatures associated with cytogenetics and prognosis in acute myeloid leukemia. *Blood* 2008;111:3183-3189.
- Wong TS, Liu XB, Chung-Wai Ho A, Po-Wing Yuen A, Wai-Man Ng R, Ignace Wei W. Identification of pyruvate kinase type M2 as potential oncoprotein in squamous cell carcinoma of tongue through microRNA profiling. *Int J Cancer* 2008;123:251-257.

Received: 2009.03.14
Accepted: 2009.05.21
Published: 2009.09.01

Authors' Contribution:

- A** Study Design
- B** Data Collection
- C** Statistical Analysis
- D** Data Interpretation
- E** Manuscript Preparation
- F** Literature Search
- G** Funds Collection

High incidence of multiple primary carcinomas in HCV-infected patients with oral squamous cell carcinoma

Yumiko Nagao^{1,ABCDEF, G}, Michio Sata^{1,2, ADE, G}

¹ Department of Digestive Disease Information & Research, Kurume University School of Medicine, Kurume, Japan
² Division of Gastroenterology, Department of Medicine, Kurume University School of Medicine, Kurume, Japan

Source of support: This study was supported in part by a Grant-in-Aid for Scientific Research (C) (No. 18592213) from the Ministry of Education, Culture, Sports, Science and Technology of Japan, and was supported in part by Health and Labour Sciences Research Grants for Research on Hepatitis from the Ministry of Health, Labour and Welfare of Japan

Background:

Hepatitis C virus (HCV) infection has been associated with several extrahepatic manifestations. Oral cancer is one of them. We investigated the association among oral squamous cell carcinoma (OSCC), multiple primary cancers (MPCs), insulin resistance and HCV infection.

Material/Methods:

Upper gastrointestinal tract examination and determination of the presence of HCV infection were routinely done for 60 primary OSCC patients. Occurrence of MPCs was evaluated between 1992 and 2008.

Results:

Of the 60 patients, 21 (35%: 15 males and 6 females; mean age 67.3±11.9 years) developed MPCs. Antibodies to HCV were found in 26.7% (16/60) of cases. The incidence of MPCs in HCV-infected OSCC cases was 62.5% (10/16 cases, P<0.01 vs the non-HCV-infected OSCC group); for cases without HCV infection it was 25% (11/44 cases). In HCV-infected cases, 10 MPCs with patients, hepatocellular carcinoma (HCC) was the most common outcome (5 cases), whereas gastric cancer was the most common outcome (6 cases) in non-HCV-infected 11 MPCs. In logistic regression analysis, the adjusted odds ratios on staging IV, anti-HCV positive, and over 70 years old were 15.50, 13.45, and 4.46, respectively, indicating that there were significant differences. Furthermore, the patients with HCV-infected MPCs had hyperinsulinemia.

Conclusions:

HCV infection was strongly associated with the occurrence of MPCs as well as primary OSCC. HCV-infected OSCC patients in Japan should receive medical treatment to inhibit development of HCC. In patients with HCV infection, it is important to clinically examine organs other than the liver.

key words:

multiple primary cancers (MPCs) • oral squamous cell carcinoma (OSCC) • hepatitis C virus (HCV) • hepatocellular carcinoma (HCC) • lichen planus • insulin resistance • extrahepatic manifestations

Abbreviations:

anti-HCV - anti-bodies to HCV; **anti-HBc** - antibody to hepatitis B core antigen;
CLEIA - chemiluminescent enzyme immunoassay; **HBsAg** - hepatitis B surface antigen;
HCC - hepatocellular carcinoma; **HCV** - hepatitis C virus; **HOMA-IR** - homeostasis model assessment; **IFN** - interferon; **MPCs** - multiple primary cancers; **OSCC** - oral squamous cell carcinoma

Full-text PDF:

<http://www.medscimonit.com/fulltxt.php?l5CID=878175>

Word count:

2612

Tables:

4

Figures:

1

References:

30

Author's address:

Yumiko Nagao, Department of Digestive Disease Information & Research, Kurume University School of Medicine, 67 Asahi-machi, Kurume 830-0011, Japan, e-mail: nagao@med.kurume-u.ac.jp



BACKGROUND

The development of multiple primary cancers (MPCs) is frequently detected in patients with oral squamous cell carcinoma (OSCC). Patients with OSCC are at risk of developing second cancers or MPCs, particularly at sites within the upper digestive tract and airway [1,2]. Routine upper gastrointestinal panendoscopy identifies synchronous MPCs in 9–14% of patients [3].

In recent years in Japan, there has been an upward trend in MPCs in patients with head and neck cancer [4]. The reasons behind this are increases in carcinoma itself, progress in diagnostic techniques, improvements in treatment outcomes, and increased mean survival time.

Since 1981, malignant neoplasms have been the leading cause of death in Japan. During the past 20 years, primary liver cancer, 95% of which is hepatocellular carcinoma (HCC), has ranked third in men and fifth in women in Japan as the cause of death from malignant neoplasms [5]. The number of deaths from HCC is expected to increase by 2010–15 [6]. Of the HCC cases in Japan, ~16% are caused by hepatitis B virus (HBV) infection and ~80% by hepatitis C virus (HCV) infection. The increase in incidence of HCC in Japan has largely been attributable to HCV infection. Geographically, HCC is more frequent in western than eastern Japan.

HCV infection has also been associated with extrahepatic manifestations and immune-mediated phenomena [7]. For example, HCV is associated with the development of OSCC. We reported for the first time an association between HCV and OSCC [8], and provided evidence, at the national level in Japan, for the high prevalence of HCV infection in patients with OSCC [9]. The subjects included 305 patients with OSCC and 276 patients with non-malignant disease (the control group) from five geographically-distinct institutions. The incidence of HCV infection in Japanese OSCC patients has been reported as 16.7–24.0% [8,9]. We also investigated the prevalence of HCV infection in oral cancer patients with MPCs [10]. Of 327 patients with OSCC, 59 (18.0%) exhibited MPCs. In the OSCC patients with MPCs, serum HCV antibodies (anti-HCV) and HCV RNA were detected in 36.7% and 28.6%, respectively [10].

Meanwhile, insulin resistance emerges as a very important host factor in patients with chronic hepatitis C. Hyperinsulinaemia is associated with accelerated HCC growth [11]. We concluded that HCV infection induces insulin resistance, which causes an increase in the incidence of extrahepatic manifestations such as lichen planus in HCV-infected individuals [12,13]. Lichen planus is an inflammatory disease of the skin and oral mucosa. The HCV infection rates in lichen planus patients are high especially in Japan [14]. Oral lichen planus should be considered as a precancerous lesion, particularly in patients presenting HCV infection [15]. Prevalence of smoking history, presence of hypertension, extrahepatic malignant tumor, and insulin resistance were significantly higher in 17 patients with lichen planus than in 70 patients without lichen planus [13].

In the current study, we surveyed the incidence of MPCs in OSCC patients with or without HCV infection and investigated the relationship between OSCC and insulin resistance.

MATERIAL AND METHODS

Subjects

This retrospective study included 60 primary OSCC patients who had visited our clinic at the Kurume University Hospital in Japan for the first time between November 1992 and December 1994. The 60 patients with OSCC included 39 males and 21 females. Their ages ranged from 32 to 85 years, with an average age of 64.8 ± 13.7 years. These patients resided in the northern Kyushu region of Japan where the prevalence of HCV infection is the highest in the country [5,16]. The stages of OSCC were as follows; stage I (15 cases), II (24), III (6), and IV (15).

MPCs were identified according to the definition proposed by Warren and Gates: there must be histological evidence of malignancy in each tumor; they must be separated from each other by normal tissue, and one tumor must not be a metastasis of another [17]. Patients with multiple OSCCs were excluded from the study. MPCs detected <6 months after OSCC diagnosis were defined as synchronous; those detected >6 months after diagnosis were defined as metachronous [17].

Methods

Upper gastrointestinal tract examinations were routinely performed in all OSCC patients using an endoscope. This was done on the first visit or first day of medical treatment in order to confirm the presence of MPCs such as carcinomas of the larynx, pharynx, esophagus, and stomach regardless of whether symptoms were present.

Sera from all 60 OSCC patients were used for the following liver function tests at the time of the first visit to our hospital: serum aspartate aminotransferase (AST), alanine aminotransferase (ALT), gammaglutamyl transpeptidase (γ -GTP), lactate dehydrogenase (LDH), total protein (TP), and albumin (Alb). Sera were also examined for the presence or absence of HCV or HBV infection. Anti-HCV antibodies and hepatitis B virus surface antigen (HBsAg) were measured by a chemiluminescent enzyme immunoassay (CLEIA) kit and a chemiluminescent immunoassay (CLIA), respectively. In 59 of 60 patients, HCV RNA in serum was detected using the Amplicore HCV test. In 58 of 60 patients, antibody to hepatitis B core antigen (anti-HBc) was found using a CLEIA kit. Ultrasonographic examination for all subjects was performed in order to examine the shape of the liver and lesions occupying the liver. Computed tomography and liver biopsy were performed in some patients.

Plasma glucose levels were measured by a glucose oxidase method for all subjects and serum insulin levels were measured using a sandwich enzyme immuno assay kit (EIKEN CHEMICAL, Tokyo, Japan). Insulin resistance was calculated on the basis of fasting levels of plasma glucose and insulin, according to the homeostasis model assessment (HOMA-IR) method [18]. The formula for the HOMA-IR is: $\text{HOMA-IR} = \text{fasting glucose (mg/dL)} \times \text{fasting insulin (}\mu\text{U/mL)} / 405$.

Their district, a history of liver dysfunction, blood transfusion, alcohol consumption, and smoking at the time of the first medical examination were collected as background information; OSCC was based upon their medical record cards.



Table 1. Incidence difference of MPCs depend on the presence or absence of HCV infection.

		Anti-HCV negative n=44 (%)		Anti-HCV positive n=16 (%)		P value A versus B
Age	Mean (year) ±SD	64.3±14.5		66.1±11.0		NS
Sex	Male	30	(68.2)	9	(56.2)	NS
	Female	14	(31.8)	7	(43.8)	
MPCs	Number	11	(25.0)	10	(62.5)	p<0.01
Primary oral SCC						
	Tongue	2	(18.2)	6	(60.0)	
	Gingiva	5	(45.5)	3	(30.0)	
	Buccal mucosa	2	(18.2)	0	(0.0)	
	Sinus	1	(9.1)	0	(0.0)	
	Oropharynx	1	(9.1)	1	(10.0)	
Number of MPCs						
	Double	(81.8)		10	(100.0)	
	Triple	(9.1)		0	(0.0)	
	Quadruple	(9.1)		0	(0.0)	
Organ of MPCs						
	Stomach	6		Liver	5	
	Esophagus	2		Colon	2	
	Skin	2		Lung	1	
	Thyroid	1		Throid	1	
	Pharynx	1		Bone marrow*	1	
	Kidney	1				
	Liver	1				
	Total	14		Total	10	
Occurrence time						
	Synchronous	6		5		
	Metachronous	6**		5		

* Acute myeloid leukemia (AML); ** One patient with quadruple cancer had cancer of the gingiva-esophagus (synchronous)-skin (synchronous)-hypopharynx (metachronous). SD – standard deviation; NS – no significance.

We observed the occurrence of MPCs from the first medical examination day to the last check-up day or nearest day preceding October 17, 2008. MPCs were diagnosed based on histopathology by the pathology laboratory which collected samples from all other medical departments of our hospital; or the diagnosis was made at other medical institutions.

Furthermore, the 60 patients whom we followed were divided into four groups: (i) MPCs with HCV infection, (ii) MPCs without HCV infection, (iii) non-MPCs with HCV infection, (iv) non-MPCs without HCV infection. We examined insulin resistance in these four groups.

Statistical analysis

All data are expressed as mean ± standard error. Differences between two groups were analyzed using the Mann-Whitney

U test and the Chi-square test. Differences were judged significant for p<0.05 (two-tailed). Adjusted odds ratios were calculated using logistic regression analysis. All statistical analyses were conducted using JMP Version 6 (SAS Institute, Cary, NC, USA). The level of statistical significance was defined as 0.05.

RESULTS

Incidence of MPCs

The details of the 60 patients studied are shown in Table 1. The mean period of follow-up was 2914.6±1536.7 days. Of the 60 patients with OSCC, 21 (35%: 15 males and 6 females; mean age 67.3±11.9 years) developed MPCs. Among the 21 patients, there were a total of 24 affected organs. The affected organs were: 6 liver cases (25%), 6 stomach (25%), 2 esophagus (8.3%), 2 colon (8.3%), 2 thyroid (8.3%), 2



This copy is for personal use only - distribution prohibited.

Table 2. Background factors of 60 patients in onset of OSCC.

		Total n=60 (%)	Group A MPCs n=21 (%)	Group B Non-MPCs n=39 (%)	P value A versus B
Age	Mean (year) \pm SD	64.8 \pm 13.7	67.3 \pm 11.9	63.4 \pm 14.4	NS
Age group	20-69 years old	35 (58.3)	10 (47.6)	25 (64.1)	NS
	70 years or older	25 (41.7)	11 (52.4)	14 (35.9)	
Sex	Male	39 (65.0)	15 (71.4)	24 (61.5)	NS
	Female	21 (35.0)	6 (28.6)	15 (38.5)	
Stage	I	15 (25.0)	4 (19.0)	11 (28.2)	NS
	II	24 (40.0)	6 (28.6)	18 (46.2)	
	III	6 (10.0)	2 (9.5)	4 (10.3)	
	IV	15 (25.0)	9 (42.9)	6 (15.4)	
Period of follow-up	Mean (days) \pm SD	2914.6 \pm 1536.7	3512.3 \pm 1355.0	2675.5 \pm 1457.9	NS
History of liver dysfunction	Yes	16 (26.7)	10 (47.6)	6 (15.4)	p<0.01
	No	41 (68.3)	9 (42.9)	32 (82.1)	
	Unknown	3 (5.0)	2 (9.5)	1 (2.6)	
History of blood transfusion	Yes	7 (11.7)	5 (23.8)	2 (5.1)	p<0.05
	No	48 (80.0)	13 (61.9)	35 (89.7)	
	Unknown	5 (8.3)	3 (14.3)	2 (5.1)	
Alcohol consumption	Yes	29 (48.3)	11 (52.4)	18 (46.2)	NS
	No	29 (48.3)	10 (47.6)	19 (48.7)	
	Unknown	2 (3.3)	0 (0.0)	2 (5.1)	
Smoking history	Yes	24 (40.0)	10 (47.6)	14 (35.9)	NS
	No	34 (56.7)	11 (52.4)	23 (59.0)	
	Unknown	2 (3.3)	0 (0.0)	2 (5.1)	

OSCC – oral squamous cell carcinoma; MPCs – multiple primary cancers; SD – standard deviation, NS: no significance.

skin (8.3%), 1 pharynx (4.2%), 1 kidney (4.2%), 1 lung (4.2%), and 1 bone marrow (leukemia, 4.2%). Nineteen patients had second primary cancers: one patient had three, and one patient had four primary cancers.

Incidence of HCV infection

Anti-HCV were detected in sera from 16 of the 60 patients with oral cancer (26.7%). The diagnosis of liver disease following the development of primary OSCC included: asymptomatic HCV carrier 6.3% (1/16), past HCV infection 6.3% (1/16), chronic hepatitis C 25% (4/16), liver cirrhosis 37.5% (6/16), HCC with liver cirrhosis 18.8% (3/16), and HCC post interferon (IFN) treatment for chronic hepatitis C 6.3% (1/16). Just after we succeeded in eliminating HCV by IFN treatment, a 38-year-old man developed simultaneous HCC and OSCC. The incidence of MPCs in an HCV-infected OSCC or in a non-HCV-infected OSCC patient was 62.5% (10/16 cases, P<0.01 vs the non-HCV-infected OSCC group) and 25% (11/44), respectively. In 10 MPC patients who were HCV-infected, HCC was the most common carcinoma (5 cases); In 11 MPC patients who were not HCV-infected, gastric cancer was the most common (6 cases).

Risk factors by univariate analysis

We compared characteristics of 21 subjects who had MPCs (group A) and 70 subjects who did not have MPCs (group B). The average age in group A was 67.3 \pm 11.9 years; there were 15 males and 6 females. The average age in group B was 63.4 \pm 14.4 years; there were 24 males and 15 females. Table 2 shows clinical features of groups A and B. A history of liver dysfunction in group A was found in 10 (47.6%, p<0.01 vs group B); a history of blood transfusion in group A was found in 5 (23.8%, p<0.05 vs group B).

We analyzed for differences between these two groups in AST, ALT, ALP, γ GTP, LDH, TP, Alb, insulin, blood glucose level, and HOMA-IR. The laboratory data of both groups are shown in Table 3. Prevalence of anti-HCV antibodies was significantly higher in group A than in group B (p<0.01).

Significant differences in the development of MPCs included a history of liver dysfunction, blood transfusion, and anti-HCV positivity.



Table 3. Laboratory data of 60 patients in onset of OSCC.

		Total n=60	Group A MPCs n=21	Group B Non-MPCs n=39	P value A versus B
AST (IU/L)	(Mean ± SD)	31.1±23.5	34.6±22.4	29.1±24.1	NS
ALT (IU/L)	(Mean ± SD)	19.5±18.5	22.7±15.4	17.7±19.9	NS
ALP (IU/L)	(Mean ± SD)	15.6±2.0	33.2±2.1	7.1±1.9	NS
γ-GTP (IU/L)	(Mean ± SD)	23.4±20.5	25.5±18.7	22.3±21.3	NS
LDH (IU/L)	(Mean ± SD)	337.1±66.8	351.1±56.5	330.4±70.8	NS
TP (g/dL)	(Mean ± SD)	7.6±0.5	7.7±0.5	7.6±0.5	NS
Alb (g/dL)	(Mean ± SD)	4.0±0.4	3.9±0.3	4.0±0.4	NS
Insulin (μU/L)	(Mean ± SD)	11.9±9.4	14.1±9.0	10.8±9.5	NS
Blood glucose level (mg/dL)	(Mean ± SD)	90.9±40.6	89.8±19.3	91.5±47.7	NS
HOMA-IR	(Mean ± SD)	3.0±3.7	3.3±2.3	2.9±4.2	NS
Anti-HCV	Positive	16 (26.7%)	10 (47.6%)	6 (15.4%)	p<0.01
	Negative	44 (73.3%)	11 (52.4%)	33 (84.6%)	
HCV RNA	Positive	13 (21.7%)	7 (33.3%)	6 (15.4%)	NS
	Negative	46 (76.7%)	13 (61.9%)	33 (84.6%)	
	Uncertain	1 (1.7%)	1 (4.8%)	0 (0.0%)	
HBsAg	Positive	1 (1.7%)	0 (0.0%)	1 (2.6%)	NS
	Negative	59 (98.3%)	21 (100.0%)	38 (97.4%)	
Anti-HBc	Positive	39 (65.0%)	14 (66.7%)	25 (64.1%)	NS
	Negative	19 (31.7%)	5 (23.8%)	14 (35.9%)	
	Uncertain	2 (3.3%)	2 (9.5%)	0 (0.0%)	

SD – standard deviation; NS – no significance; AST – serum aspartate aminotransferase; ALT – alanine aminotransferase; γ-GTP – gammaglutamyl transpeptidase; LDH – lactate dehydrogenase; TP – total protein; Alb – albumin; HOMA IR – homeostasis model assessment.

Multivariate analysis

According to multivariate analysis, three factors – stage IV, anti-HCV positivity, and over 70 years old – were identified as factors associated with OSCC patients having an increased chance of developing MPCs. The adjusted odds ratios for these three factors were 15.50, 13.45, and 4.46, respectively, and each was statistically significant (Table 4).

Insulin resistance for the four groups

Of the 60 subjects (16 anti-HCV antibody positive and 44 anti-HCV negative), 10 had MPCs with HCV infection (group 1), 11 had MPCs without HCV infection (group 2), 6 lacked MPCs but had HCV infection (group 3), and 33 lacked MPCs and HCV infection (group 4). Fasting insulin levels at the time of the first visit to our hospital were: 16.3±7.9, 12.1±9.5, 13.5±12.6, or 10.3±8.7, in groups 1, 2, 3 and 4, respectively. Fasting insulin levels for group 1 was significantly higher than for group 4 (p=0.01, Figure 1A). HOMA-IR values seven years prior in groups 1, 2, 3, and 4 were, respectively, 3.5±1.6, 3.0±2.7, 3.1±3.0, and 2.9±4.4. A

Table 4. Results of multivariate analysis.

	Adjusted odds ratio (95% confidence interval)	P value
Stage IV	15.50 (0.39–2.58)	P=0.0124
Anti-HCV positive	13.45 (0.50–2.30)	P=0.0039
70 years or older	4.46 (0.04–1.56)	P=0.0480

HOMA-IR value for group 1 was significantly higher than for group 4 (p=0.01, Figure 1B).

DISCUSSION

We have already reported a high incidence of HCV among patients with OSCC [8,9]. Furthermore, we investigated the characteristics and incidence of MPCs in patients with OSCC treated between 1974 and 1995, suggesting that HCV infection increases the risk of developing MPCs [10].



This copy is for personal use only - distribution prohibited.

CR

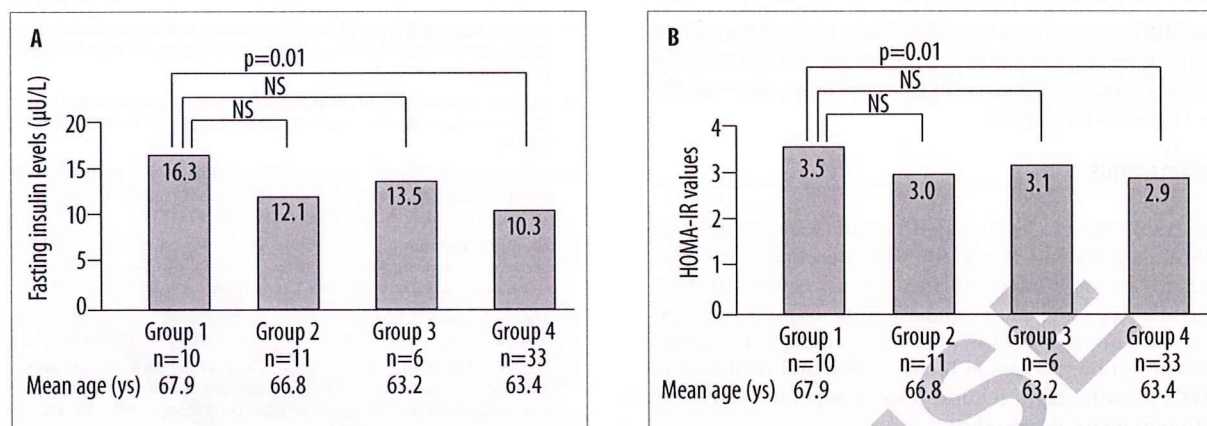


Figure 1. Association of carcinomas with insulin resistance depend on the presence or absence of OSCC and HCV infection. (A) Fasting serum insulin levels and (B) HOMA-IR values.

In the present study, the incidence of MPCs in patients with OSCC was 35% (21/60 patients) during 2914.6±1536.7 days of follow-up. The incidence of anti-HCV positivity was 26.7% (16/60 patients). The incidence of MPCs in an OSCC patient that was HCV-infected was significantly higher than in one that was not infected (62.5% vs 25%, $p < 0.01$). HCC was the most common form of HCV-infected MPCs, and gastric cancer was the most common form of non-HCV-infected MPCs. These findings suggest a strong association between HCV infection and OSCC. The incidence of MPCs with the exclusion of 5 HCC in an OSCC patient that was HCV-infected was also higher than in one that was not infected (45.1% vs 25%). The affected carcinomas in extrahepatic organs of OSCC patients with HCV infection were: 2 colons, 1 lung, 1 thyroid, and 1 bone marrow (leukemia). Even excluding HCC, HCV-infected patients were at a high risk of developing extrahepatic MPCs.

Multivariate analysis demonstrated that stages of OSCC, being anti-HCV positive, and being over 70 years old increased the risk that patients with OSCC would develop MPCs. In OSCC patients who are HCV-infected, it is important to clinically examine the liver other than the oral cavity and gastrointestinal regions.

HCV infection induces not only chronic liver disease but also extrahepatic manifestations. Indeed, we experienced and reported five head and neck SCC among HCV-infected patients: (i) the patient who developed buccal mucosa cancer after IFN therapy for chronic hepatitis C [19], (ii) the patient who had simultaneous double primary cancers, including tongue cancer and HCV-related HCC [20], (iii) the patient who developed tongue cancer during the treatment of HCV-related liver disease [20], (iv) the patient with chronic hepatitis C, who developed worsening of lichen planus lesions during treatment with IFN plus ribavirin [21] and subsequently developed larynx cancer, and (v) the patient who developed tongue cancer during treatment for chronic hepatitis C [22].

It is presumed that between 1 and 2 million Japanese people are chronically infected with HCV. Because many such people are unaware that they are infected, carriers may develop liver cirrhosis and HCC, and this poses a serious problem. HCV-related HCC has increased and is now the cause

of a majority of cases in Japan. Thus, the increased rates of death due to primary liver cancer in Japan appear to reflect the increase in numbers of HCV-related HCC [5]. IFN therapy, an antiviral agent, contributes to the prevention of occurrence of HCC and to improvement in long-term prognosis [23,24]. HCV-infected OSCC patients should also receive medical treatment to inhibit development of HCC, especially in Japan where the average life expectancy has increased year after year. In 2006, the life expectancies at birth were 79.0 years for males and 85.8 for females (Abridged Life Table, Ministry of Health, Labour and Welfare). Meanwhile, in patients with HCV infection, it is important to clinically examine organs other than the liver.

Satoh et al reported autopsy cases collected from the Annual of the Pathological Autopsy Cases in Japan, which is issued by the Japanese Society of Pathology for the past five years 1997–2001 [4]. A total of 134,997 cases had autopsies in Japan over five years. Of these, 321 were tongue cancer. The incidence of MPCs, affecting both the tongue and other organs, was reported to be 35.2% (113/321). In cases of double cancers including tongue cancer, commonly occurring cancers were reported to be lung, liver, esophagus, and thyroid. We think that there is a strong relation between OSCC and HCV infection, as can be seen from the fact that the second most common MPCs with tongue cancer, according to the results of autopsies, is liver cancer (reported by Satoh et al).

Several studies and our previous reports suggest that HCV infection antedates insulin resistance [25,26]. We showed molecular mechanisms for HCV core-induced insulin resistance [26]. Meanwhile, in a large population-based cohort study, Park et al. reported that among male cancer survivors, prediagnosis smoking, alcohol consumption, obesity, and insulin resistance (all risk factors for cancer development) affected cancer prognosis [27]. Previous studies in breast, prostate, and colorectal cancers demonstrated that insulin resistance can influence outcomes through systemic consequences of hyperinsulinemia [28–30]. Insulin receptors are overexpressed in those cancer tissues, so high insulin levels could promote the selective growth advantage of cancer cells [28–30]. We conclude that HCV infection induces insulin resistance and may cause lichen planus, a precancerous lesion [12,13]. In the present study,

the MPC patients who were HCV-infected had hyperinsulinemia. Insulin resistance may be involved in the development of MPCs in patients with HCV infection, although the mechanisms are unclear.

CONCLUSIONS

We demonstrated a high incidence of MPCs in HCV-infected OSCC patients. Risk factors for MPCs developing in OSCC patients are high stage of primary cancer, HCV infection, and older age. Our study emphasizes the importance of periodic examination of the oral cavity among patients with HCV infection. Success in the detection and treatment of MPCs at early stages requires close cooperation between different medical specialists.

REFERENCES:

- Day GL, Blot WJ: Second primary tumors in patients with oral cancer. *Cancer*, 1992; 70: 14-19
- Crosher R, McIlroy R: The incidence of other primary tumours in patients with oral cancer in Scotland. *Br J Oral Maxillofac Surg*, 1998; 36: 58-62
- Licciardello JT, Spitz MR, Hong WK: Multiple primary cancer in patients with cancer of the head and neck: second cancer of the head and neck, esophagus, and lung. *Int J Radiat Oncol Biol Phys*, 1989; 17: 467-76
- Satoh M, Oikawa Y, Furiya I: A statistical study of autopsy cases of tongue cancer in Japan (Part VI) (in Japanese). *Dent J Iwate Med Univ*, 2005; 30: 53-64
- Kiyosawa K, Uemura T, Ichijo T et al: Hepatocellular Carcinoma: Recent Trends in Japan. *Gastroenterology*, 2004; 127 (5 Suppl.1): 17-26
- Shibuya K, Yano E: Regression analysis of trends in mortality from hepatocellular carcinoma in Japan, 1972-2001. *Int J Epidemiol*, 2005; 34: 397-402
- Pawlotsky JM, Ben Yahia M, Andre C et al: Immunological disorders in C virus chronic active hepatitis: A prospective case-control study. *Hepatology*, 1994; 19: 841-48
- Nagao Y, Sata M, Tanikawa K et al: High prevalence of hepatitis C virus antibody and RNA in patients with oral cancer. *J Oral Pathol Med*, 1995; 24: 354-60
- Nagao Y, Sata M, Itoh K et al: High prevalence of hepatitis C virus antibody and RNA in patients with head and neck squamous cell carcinoma. *Hepatol Res*, 1997; 7: 206-12
- Yoshida M, Nagao Y, Sata M et al: Multiple primary neoplasms and hepatitis C virus infection in oral cancer patients. *Hepatol Res*, 1997; 9: 75-81
- Saito K, Inoue S, Saito T et al: Augmentation effect of postprandial hyperinsulinaemia on growth of human hepatocellular carcinoma. *Gut*, 2002; 51: 100-4
- Nagao Y, Kawaguchi T, Tanaka K et al: Extrahepatic manifestations and insulin resistance in an HCV hyperendemic area. *Int J Mol Med*, 2005; 16: 291-96
- Nagao Y, Kawasaki K, Sata M: Insulin resistance and lichen planus in patients with HCV-infectious liver diseases. *J Gastroenterol Hepatol*, 2008; 23: 580-85
- Nagao Y, Sata M, Tanikawa K et al: Lichen planus and hepatitis C virus in the northern Kyushu region of Japan. *Eur J Clin Invest*, 1995; 25: 910-14
- Gandolfo S, Richiardi L, Carrozzo M et al: Risk of oral squamous cell carcinoma in 402 patients with oral lichen planus: a follow-up study in an Italian population. *Oral Oncol*, 2002; 40: 77-83
- Hayashi J, Yoshimura E, Nabeshima A et al: Seroepidemiology of hepatitis C virus infection in hemodialysis patients and the general population in Fukuoka and Okinawa, Japan. *J Gastroenterol*, 1994; 29: 276-81
- Warren S, Gates O: Multiple primary malignant tumors. A survey of the literature and statistical study. *Am J Cancer*, 1932; 16: 1358-414
- Matthews DR, Hosker JP, Rudenski AS et al: Homeostasis model assessment: insulin resistance and beta-cell function from fasting plasma glucose and insulin concentrations in man. *Diabetologia*, 1985; 28: 412-19
- Nagao Y, Sata M, Fukuizumi K et al: Oral cancer and hepatitis C virus (HCV): can HCV alone cause oral cancer? – a case report. *Kurume Med J*, 1996; 43: 97-100
- Nagao Y, Sata M, Noguchi S et al: Various extrahepatic manifestations caused by hepatitis C virus infection. *Int J Mol Med*, 1999; 4: 621-25
- Nagao Y, Kawaguchi T, Ide T et al: Exacerbation of oral erosive lichen planus by combination of interferon and ribavirin therapy for chronic hepatitis C. *Int J Mol Med*, 2005; 15: 237-41
- Nagao Y, Hiromatsu Y, Nakashima T, Sata M: Graves' ophthalmopathy and tongue cancer complicated by peg-interferon α -2b and ribavirin therapy for chronic hepatitis C: A case report and review of the literature. *Molecular Medicine Reports*, 2008; 1: 625-31
- Yoshida H, Shiratori Y, Moriyama M et al: Interferon therapy reduces the risk for hepatocellular carcinoma: national surveillance program of cirrhotic and noncirrhotic patients with chronic hepatitis C in Japan. IHIT Study Group. Inhibition of Hepatocarcinogenesis by Interferon Therapy. *Ann Intern Med*, 1999; 131: 174-81
- Yoshida H, Arakawa Y, Sata M et al: Interferon therapy prolonged life expectancy among chronic hepatitis C patients. *Gastroenterology*, 2002; 123: 483-91
- Hui JM, Sud A, Farrell GC et al: Insulin resistance is associated with chronic hepatitis C and virus infection fibrosis progression. *Gastroenterology*, 2003; 125: 1695-704
- Kawaguchi T, Yoshida T, Harada M et al: Hepatitis C virus down-regulates insulin receptor substrates 1 and 2 through up-regulation of suppressor of cytokine signaling 3. *Am J Pathol*, 2004; 165: 1499-508
- Park SM, Lim MK, Shin SA, Yun YH: Impact of prediagnosis smoking, alcohol, obesity, and insulin resistance on survival in male cancer patients: National Health Insurance Corporation Study. *J Clin Oncol*, 2006; 24: 5017-24
- Jee SH, Ohrr H, Sull JW et al: Fasting serum glucose level and cancer risk in Korean men and women. *JAMA*, 2005; 293: 194-202
- Dawson SI: Long-term risk of malignant neoplasm associated with gestational glucose intolerance. *Cancer*, 2004; 100: 149-55
- Hsing AW, Gao YT, Chua S Jr et al: Insulin resistance and prostate cancer risk. *J Natl Cancer Inst*, 2003; 95: 67-71



LETTERS

Endogenous non-retroviral RNA virus elements in mammalian genomes

Masayuki Horie^{1*}, Tomoyuki Honda^{1,2*}, Yoshiyuki Suzuki³, Yuki Kobayashi³, Takuji Daito¹, Tatsuo Oshida⁴, Kazuyoshi Ikuta¹, Patric Jern⁵, Takashi Gojobori³, John M. Coffin⁵ & Keizo Tomonaga^{1,6}

Retroviruses are the only group of viruses known to have left a fossil record, in the form of endogenous proviruses, and approximately 8% of the human genome is made up of these elements^{1,2}. Although many other viruses, including non-retroviral RNA viruses, are known to generate DNA forms of their own genomes during replication^{3–5}, none has been found as DNA in the germline of animals. Bornaviruses, a genus of non-segmented, negative-sense RNA virus, are unique among RNA viruses in that they establish persistent infection in the cell nucleus^{6–8}. Here we show that elements homologous to the nucleoprotein (N) gene of bornavirus exist in the genomes of several mammalian species, including humans, non-human primates, rodents and elephants. These sequences have been designated endogenous Borna-like N (EBLN) elements. Some of the primate EBLNs contain an intact open reading frame (ORF) and are expressed as mRNA. Phylogenetic analyses showed that EBLNs seem to have been generated by different insertional events in each specific animal family. Furthermore, the EBLN of a ground squirrel was formed by a recent integration event, whereas those in primates must have been formed more than 40 million years ago. We also show that the N mRNA of a current mammalian bornavirus, Borna disease virus (BDV), can form EBLN-like elements in the genomes of persistently infected cultured cells. Our results provide the first evidence for endogenization of non-retroviral virus-derived elements in mammalian genomes and give novel insights not only into generation of endogenous elements, but also into a role of bornavirus as a source of genetic novelty in its host.

Bornaviruses are the only animal RNA viruses that achieve a highly cell-associated life cycle within the nuclear envelope^{6–9}, and can therefore provide not only new models of RNA virus replication, but also insight into dynamics of RNA molecules in eukaryote cells. In an effort to understand whether bornaviruses mimic host factors to maintain persistent infection in the nucleus, we searched human protein databases for sequences with similarity to BDV proteins. This search identified two hypothetical human proteins (GeneID LOC340900 and LOC55096), each of which has significant sequence similarity to BDV N (Fig. 1a and Supplementary Table 1). BDV N is a major structural protein, which tightly encapsidates the viral RNA to form the nucleocapsid. The LOC340900 sequence encodes a protein of comparable length (366 residues) to BDV N (370 residues), whereas LOC55096 seems to contain several frameshift mutations relative to BDV N, resulting in a shorter ORF length (Fig. 1a). Both LOC340900 and LOC55096 showed an overall 41% sequence identity and 58% similarity to BDV N and 72% identity to each other. The close relationship between BDV N and the homologous genes was

further demonstrated by the alignment of transcription regulatory sequences on either side of BDV N (Fig. 1b). The S and T motifs in flanking sequences of both putative human proteins were well conserved with those of BDV (Fig. 1b). In addition, a poly-A sequence appears after the T1-like motif in the 3' flanking region of LOC55096 (Fig. 1b). The homology of the human genes to BDV N was also confirmed by a permutation test (Supplementary Fig. 1). These findings indicated that both human genes may be endogenous elements related to BDV N gene, and therefore we designated them EBLNs (LOC340900, EBLN-1 and LOC55096, EBLN-2).

To investigate the presence of EBLN sequences in other animal species, we conducted *tblastn* searches using BDV N as a query in eukaryote and whole-genome shotgun databases at NCBI. Sequences with blast *E*-values of 10^{-10} or lower were identified as EBLNs. We found two additional human elements (EBLN-3 and -4) as well as a number of related sequences in various mammalian species, including marsupials (Supplementary Table 2). Orthologous genes to human EBLNs were identified in the genomes of non-human anthropoid primates, including chimpanzee, gorilla, orang-utan, and macaque (Supplementary Table 2). We also detected primate EBLNs in the genomes of the suborder Strepsirrhini, including the mouse lemur and Garnett's galago. Furthermore, two species of the Afrotheria, African elephant and cape hyrax, and four rodents were found to have EBLNs with *E*-values of less than 10^{-20} (Supplementary Table 2). An EBLN locus with a high level of similarity to BDV N was also identified in the thirteen-lined ground squirrel (TLS) genome (Supplementary Fig. 2a). Like the human EBLNs, the TLS EBLN contained a 3' poly-A sequence, as well as S and T signal motifs, in its 3' flanking region (Supplementary Fig. 2b). Almost all EBLN fragments, except for EBLN-1 and the TLS gene, contained several stop codons in the predicted coding sequences, or lacked the identifiable flanking sequences. In addition, we found that all anthropoid EBLNs, except for EBLN-4, are expressed as mRNAs in some human and monkey-derived cell lines (Supplementary Fig. 3). A previous study reported the interaction of human EBLN-2 with other cellular proteins, such as AP1S1, TUSC2/FUS1 and FANCC (ref. 10) (Supplementary Table 1), indicating that anthropoid EBLNs may encode functional proteins.

To investigate whether other mammalian species contain EBLN-related sequences in their genomes further, we conducted Southern blot hybridization under low-stringency conditions using human, murine and TLS EBLN as probes (Fig. 1c and d). Along with the clear signals in primate genomes, we detected reproducible faint positive bands in murine and shrew genomes when using a human EBLN probe (Fig. 1c, dots). The signals were also observed using a mouse

¹Department of Virology, Research Institute for Microbial Diseases (BIKEN), Osaka University, Osaka 565-0871, Japan. ²Japan Society for the Promotion of Science (JSPS), Chiyoda-ku, Tokyo 102-8472, Japan. ³Center for Information Biology and DNA Data Bank of Japan, National Institute of Genetics, Mishima, Shizuoka 411-8540, Japan. ⁴Department of Life Science and Agriculture, Obihiro University of Agriculture and Veterinary Medicine, Obihiro, Hokkaido 080-8555, Japan. ⁵Department of Molecular Biology and Microbiology, Tufts University School of Medicine, Boston, Massachusetts 02111, USA. ⁶PRESTO, Japan Science and Technology Agency (JST), Chiyoda-ku, Tokyo 102-0075, Japan. *These authors contributed equally to this work.

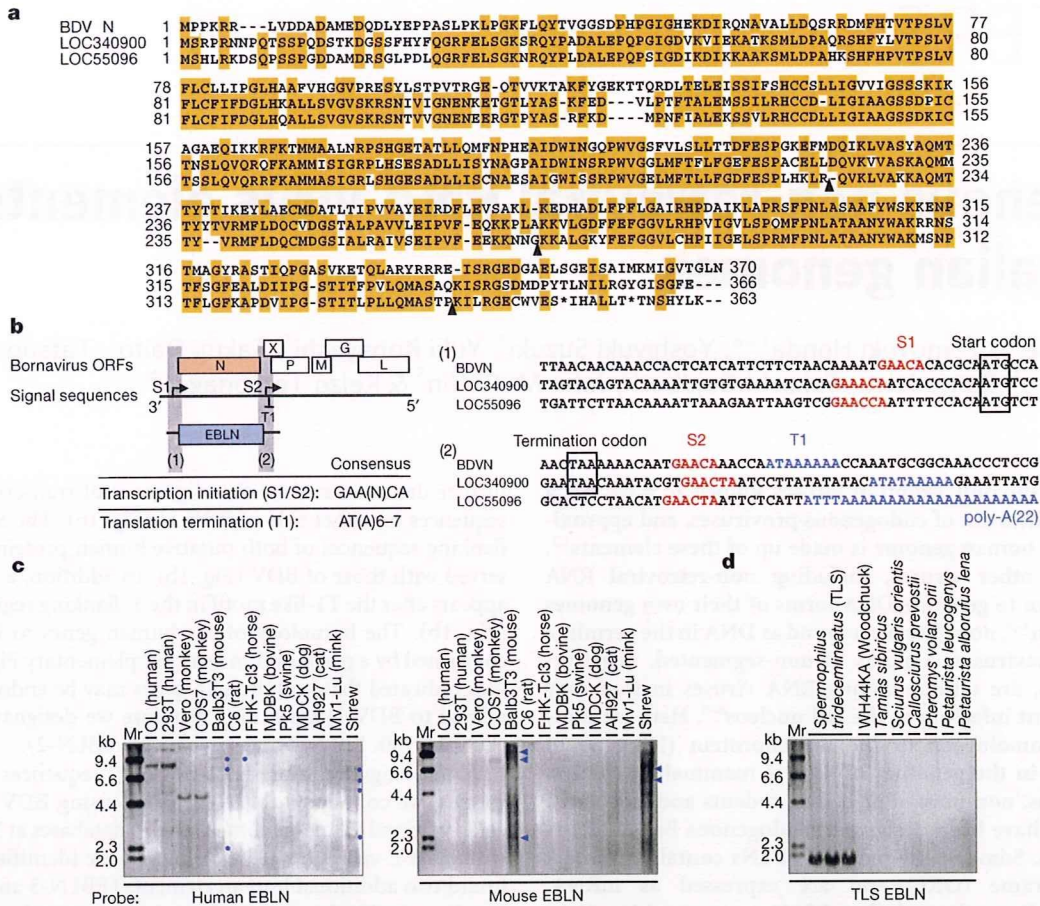


Figure 1 | Bornavirus N-like elements in mammalian genomes.

a, Alignment between predicted amino acid sequences of BDV N and two human bornavirus N-like elements. Black arrowheads indicate predicted frameshift sites in LOC55096. **b**, Sequence alignments of transcription signal sites (S1/S2 and T1) at both the 5' and 3' ends of the bornavirus N ORF. A schematic representation of bornavirus genome structure is shown.

EBLN probe (Fig. 1c, arrowheads), indicating that the faint bands are most likely to be EBLN-related sequences. In fact, EBLN-like sequences, albeit with *E*-values greater than 10^{-10} , were found in the Eurasian shrew genome in our tblastn searches. On the other hand, except for TLS, no positive band was detected by the TLS probe in the genomes of several different squirrel species, such as woodchuck (*Marmota* spp.), the closest species to the TLS (*Spermophilus* spp.) (Fig. 1d)¹¹, indicating that the ground squirrels are likely to be the only host species of EBLN within the squirrel family. The BDV N probe detected many faint and smear bands that include the signals detected by EBLN-specific probes in both selected mammalian species and the squirrel families (Supplementary Fig. 4), indicating that EBLN-related fragments are more widely distributed in the mammalian genome.

We next performed a comprehensive phylogenetic analysis using nucleotide sequences of all EBLNs with *E*-values less than 10^{-20} (Fig. 2 and Supplementary Fig. 5). In addition to EBLNs, we included avian bornaviruses (ABVs)¹² and an exogenous reptile bornavirus (RBV) sequence, which was detected in a cDNA library from a *Bitis gabonica* (Gaboon viper) venom gland¹³ (Supplementary Fig. 6). As shown in Fig. 2, the anthropoid and murine EBLNs are clustered phylogenetically within each host order. By contrast, EBLNs from other species, including African elephant, cape hyrax and guinea pig, form branches independent from the evolutionary lineage of their hosts, indicating that these EBLNs had most likely invaded each species via independent integration events. Interestingly, the TLS EBLNs form a tight cluster more closely related to modern exogenous bornaviruses than to those of other animals. Considering that a closely related species does not contain EBLNs, the integration of squirrel EBLN could have been a very

c, d, Low-stringency Southern blot hybridizations of DNA from various mammalian species using human EBLN-1 and mouse EBLN chr.11 (**c**) and TLS EBLN (**d**) as probes. Dots and arrowheads on the right side of the murine and shrew lanes in panel **c** indicate the positions of reproducible positive signals. Mr, Molecular marker.

recent event. A phylogenetic analysis using all primate EBLNs, including marmoset (Supplementary Fig. 7), showed that the integration events leading to the primate EBLNs occurred in the Haplorrhini at least before the split between rhesus macaque and marmoset.

To investigate whether current bornaviruses are able to be copied into DNA to produce EBLN-like elements, we first performed PCR analyses using DNA of persistently BDV-infected cells. As shown in Fig. 3a and Supplementary Table 3, BDV DNA was clearly detected in some cell lines by a primer set targeted to the BDV N region. To understand which viral RNA species serve as template for the DNA form of BDV, we used several primers within the BDV genome for amplification. The results showed that primer sets straddling the boundaries of BDV transcription units could not amplify BDV-specific DNA (Fig. 3b and c), indicating that the DNA is transcribed from mRNAs of BDV. We detected BDV-specific DNA in the brains of persistently BDV-infected mice (Supplementary Fig. 8), indicating that BDV can produce DNA forms *in vitro* and *in vivo*. We next performed Alu-PCR to investigate whether BDV DNA detected in the infected cells exists as integrated or extrachromosomal DNA. As shown in Fig. 3d and Supplementary Fig. 9, an Alu-specific PCR product was detected in BDV-infected cells only when using an N-specific forward primer about 30 days post-infection. This observation indicated that although BDV DNA in infected cells may be mainly extrachromosomal, the N gene is integrated into the host genome during persistent infection.

We further characterized the BDV DNA insertions and flanking cellular sequences by using Alu-PCR and inverse PCR (Supplementary Fig. 10)¹⁴. Integration sites were present on various chromosomes

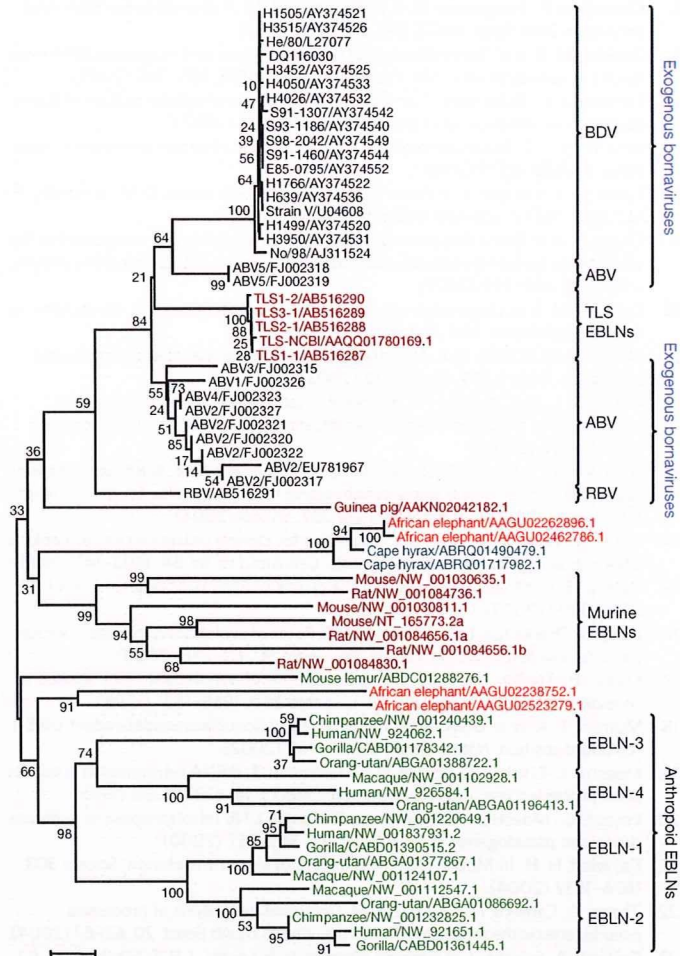


Figure 2 | Phylogenetic tree of exogenous bornaviruses and mammalian EBLNs. The bootstrap probability is indicated for each interior branch. The scale bar indicates the number of amino acid substitutions per site. Animals belonging to the same order are indicated by the same colour. Strain and sequence accession numbers are given for each sequence.

(Fig. 4). Similar to some mammalian EBLNs, many BDV DNA insertions contained a 3' poly-A sequence (Fig. 4b and c). In addition, integrations of truncated BDV N DNA were also found in some clones. No apparent consensus sequences were found at the sites, although target site duplications (TSDs) were detected in some clones from the inverse PCR (Fig. 4c). We also found deletions, as well as sequence rearrangement, of host genome adjacent to BDV DNA insertions (Fig. 4c). These results indicate that modern BDV is able to produce DNA forms leading to insertion of EBLN-like elements into its host's genome.

This report is the first to provide evidence of endogenous sequences derived from a non-retroviral RNA virus in mammalian species. Phylogenetic analyses demonstrate that the oldest primate EBLN observed must have appeared in an ancestor of primates after the separation between Strepsirrhini and Haplorrhini, implying that bornaviruses have coexisted with primates for an evolutionary history stretching at least 40 million years. Thus, bornaviruses are the first non-retroviral RNA virus whose existence in prehistoric times has been confirmed. To date, the evolution/origin of RNA viruses is a major puzzle in the relationship between viruses and mammalian hosts, because simple molecular clock calculations using an average rate of nucleotide substitutions estimate the origin of RNA viruses to be a very recent event^{15–17}. Despite replication during tens of millions of years as exogenous viruses, the amino acid sequences of current BDV N seem surprisingly conserved relative to EBLNs. This conservation demonstrates the inapplicability of simple molecular clocks to RNA virus evolution. Discovery of EBLNs in several

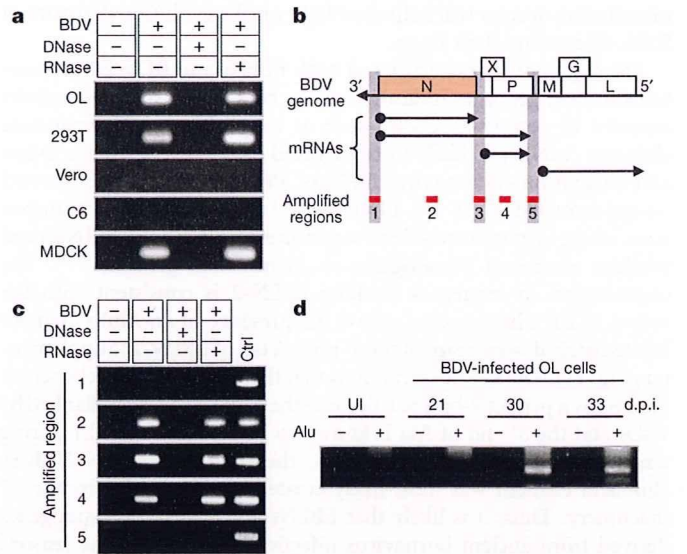


Figure 3 | Reverse transcription and integration of BDV RNA in mammalian cells. **a**, PCR amplification of BDV N-specific cDNA in BDV-infected cells. OL and 293T, human; Vero, monkey; C6, rat; MDCK, dog. **b**, Schematic representation of the bornavirus genome and mRNAs. Regions for the PCR amplification are indicated by red bars. **c**, Region-dependent amplification of BDV cDNA in infected OL cells. The numbers on the left side of the panels correspond to the amplification regions in panel **b**. Ctrl indicates the results of RT-PCR using RNA from BDV-infected OL cells. **d**, Integration of BDV DNA. Genomic DNA was isolated from BDV-infected OL cells at the indicated days after infection, and Alu-PCR was performed with (+) or without (-) the Alu primer. UI, genomic DNA from uninfected cells; d.p.i., days post-infection.

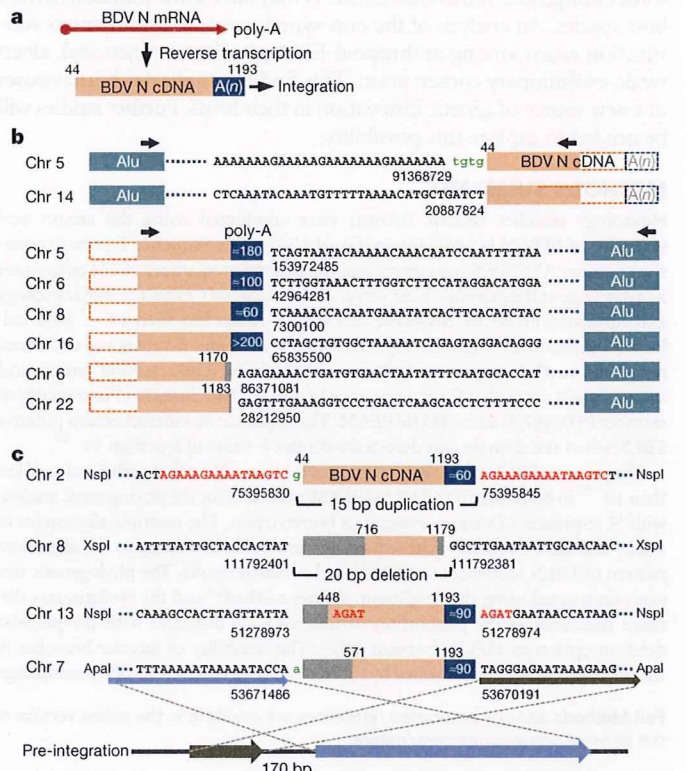


Figure 4 | Structures of BDV N integration events in OL cells. **a**, Structure of BDV N cDNA. The numbering corresponds to nucleotide positions in the BDV genome. The BDV N transcript runs from nucleotide positions 44 to 1193. **b**, **c**, Structures of BDV N integrations detected by Alu-PCR (**b**) and inverse PCR (**c**). Grey rectangles in the N cDNA indicate truncated regions. Black lettering, host genome sequences; green lettering, inserted nucleotides; red lettering, predicted TSDs. The blue box indicates the position and length of the poly-A sequence. The pre-integration form of chromosome 7 is shown in panel **c**.